Mathematical Problems in Engineering

Advanced Mathematical Models for Sustainable Policies and Technologies in the Renewable Energy Sector

Lead Guest Editor: Mohammad Reza Safaei
Guest Editors: Reza Maihami, Marjan Goodarzi, and Mikhail A Sheremet

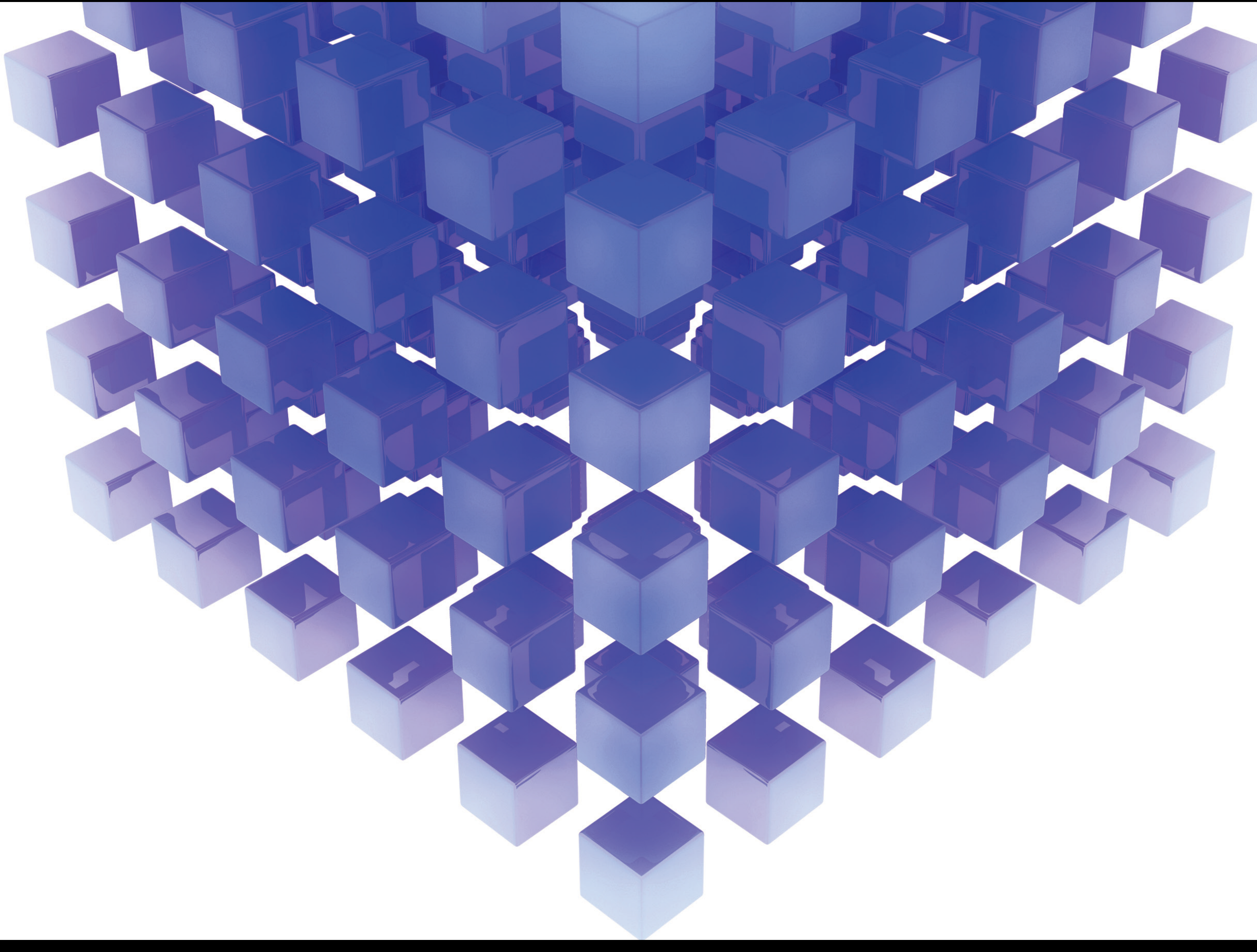

Advanced Mathematical Models for Sustainable Policies and Technologies in the Renewable Energy Sector

Mathematical Problems in Engineering

Advanced Mathematical Models for Sustainable Policies and Technologies in the Renewable Energy Sector

Lead Guest Editor: Mohammad Reza Safaei
Guest Editors: Reza Maihami, Marjan Goodarzi, and Mikhail A Sheremet

Paolo Boscariol, Italy
Daniela Boso, Italy
Guillermo Botella-Juan, Spain
Abdesselem Boulkroune, Algeria
Boulaïd Boulkroune, Belgium
Fabio Bovenga, Italy
Francesco Braghin, Italy
Ricardo Branco, Portugal
Julien Bruchon, France
Matteo Bruggi, Italy
Michele Brun, Italy
Maria Elena Bruni, Italy
Maria Angela Butturi, Italy
Bartłomiej Błachowski, Poland
Dhanamjayulu C, India
Raquel Caballero-Águila, Spain
Filippo Cacace, Italy
Salvatore Caddemi, Italy
Zuowei Cai, China
Roberto Caldelli, Italy
Francesco Cannizzaro, Italy
Maosen Cao, China
Ana Carpio, Spain
Rodrigo Carvajal, Chile
Caterina Casavola, Italy
Sara Casciati, Italy
Federica Caselli, Italy
Carmen Castillo, Spain
Inmaculada T. Castro, Spain
Miguel Castro, Portugal
Giuseppe Catalanotti, United Kingdom
Alberto Cavallo, Italy
Gabriele Cazzulani, Italy
Fatih Vehbi Celebi, Turkey
Miguel Cerrolaza, Venezuela
Gregory Chagnon, France
Ching-Ter Chang, Taiwan
Kuei-Lun Chang, Taiwan
Qing Chang, USA
Xiaoheng Chang, China
Prasenjit Chatterjee, Lithuania
Kacem Chehdi, France
Peter N. Cheimets, USA
Chih-Chiang Chen, Taiwan
He Chen, China
Kebing Chen, China
Mengxin Chen, China
Shyi-Ming Chen, Taiwan
Xizhong Chen, Ireland
Xue-Bo Chen, China
Zhiwen Chen, China
Qiang Cheng, USA
Zeyang Cheng, China
Luca Chiapponi, Italy
Francisco Chicano, Spain
Tirivanhu Chinyoka, South Africa
Adrian Chmielewski, Poland
Seongim Choi, USA
Gautam Choubey, India
Hung-Yuan Chung, Taiwan
Yusheng Ci, China
Simone Cinquemani, Italy
Roberto G. Citarella, Italy
Joaquim Ciurana, Spain
John D. Clayton, USA
Piero Colajanni, Italy
Giuseppina Colicchio, Italy
Vassilios Constantoudis, Greece
Enrico Conte, Italy
Alessandro Contento, USA
Mario Cools, Belgium
Gino Cortellessa, Italy
Carlo Cosentino, Italy
Paolo Crippa, Italy
Erik Cuevas, Mexico
Guozeng Cui, China
Mehmet Cunkas, Turkey
Giuseppe D'Aniello, Italy
Peter Dabnichki, Australia
Weizhong Dai, USA
Zhifeng Dai, China
Purushothaman Damodaran, USA
Sergey Dashkovskiy, Germany
Adiel T. De Almeida-Filho, Brazil
Fabio De Angelis, Italy
Samuele De Bartolo, Italy
Stefano De Miranda, Italy
Filippo De Monte, Italy

José António Fonseca De Oliveira Correia, Portugal
Jose Renato De Sousa, Brazil
Michael Defoort, France
Alessandro Della Corte, Italy
Laurent Dewasme, Belgium
Sanku Dey, India
Gianpaolo Di Bona, Italy
Roberta Di Pace, Italy
Francesca Di Puccio, Italy
Ramón I. Diego, Spain
Yannis Dimakopoulos, Greece
Hasan Dinçer, Turkey
José M. Domínguez, Spain
Georgios Dounias, Greece
Bo Du, China
Emil Dumic, Croatia
Madalina Dumitriu, United Kingdom
Premraj Durairaj, India
Saeed Eftekhar Azam, USA
Said El Kafhali, Morocco
Antonio Elipe, Spain
R. Emre Erkmen, Canada
John Escobar, Colombia
Leandro F. F. Miguel, Brazil
FRANCESCO FOTI, Italy
Andrea L. Facci, Italy
Shahla Faisal, Pakistan
Giovanni Falsone, Italy
Hua Fan, China
Jianguang Fang, Australia
Nicholas Fantuzzi, Italy
Muhammad Shahid Farid, Pakistan
Hamed Faroqi, Iran
Yann Favennec, France
Fiorenzo A. Fazzolari, United Kingdom
Giuseppe Fedele, Italy
Roberto Fedele, Italy
Baowei Feng, China
Mohammad Ferdows, Bangladesh
Arturo J. Fernández, Spain
Jesus M. Fernandez Oro, Spain
Francesco Ferrise, Italy
Eric Feulvarch, France
Thierry Floquet, France
Eric Florentin, France
Gerardo Flores, Mexico
Antonio Forcina, Italy
Alessandro Formisano, Italy
Francesco Franco, Italy
Elisa Francomano, Italy
Juan Frausto-Solis, Mexico
Shujun Fu, China
Juan C. G. Prada, Spain
HECTOR GOMEZ, Chile
Matteo Gaeta, Italy
Mauro Gaggero, Italy
Zoran Gajic, USA
Jaime Gallardo-Alvarado, Mexico
Mosè Gallo, Italy
Akemi Gálvez, Spain
Maria L. Gandarias, Spain
Hao Gao, Hong Kong
Xingbao Gao, China
Yan Gao, China
Zhiwei Gao, United Kingdom
Giovanni Garcea, Italy
José García, Chile
Harish Garg, India
Alessandro Gasparetto, Italy
Stylianos Georgantzinos, Greece
Fotios Georgiades, India
Parviz Ghadimi, Iran
Ştefan Cristian Gherghina, Romania
Georgios I. Giannopoulos, Greece
Agathoklis Giaralis, United Kingdom
Anna M. Gil-Lafuente, Spain
Ivan Giorgio, Italy
Gaetano Giunta, Luxembourg
Jefferson L.M.A. Gomes, United Kingdom
Emilio Gómez-Déniz, Spain
Antonio M. Gonçalves de Lima, Brazil
Qunxi Gong, China
Chris Goodrich, USA
Rama S. R. Gorla, USA
Veena Goswami, India
Xunjie Gou, Spain
Jakub Grabski, Poland

Irfan Kaymaz, Turkey
Vahid Kayvanfar, Qatar
Krzysztof Kecik, Poland
Mohamed Khader, Egypt
Chaudry M. Khalique, South Africa
Mukhtaj Khan, Pakistan
Shahid Khan, Pakistan
Nam-Il Kim, Republic of Korea
Philipp V. Kiryukhantsev-Korneev, Russia
P.V.V Kishore, India
Jan Koci, Czech Republic
Ioannis Kostavelis, Greece
Sotiris B. Kotsiantis, Greece
Frederic Kratz, France
Vamsi Krishna, India
Edyta Kucharska, Poland
Krzysztof S. Kulpa, Poland
Kamal Kumar, India
Prof. Ashwani Kumar, India
Michal Kunicki, Poland
Cedrick A. K. Kwuimy, USA
Kyandoghere Kyamakya, Austria
Ivan Kyrchei, Ukraine
Márcio J. Lacerda, Brazil
Eduardo Lalla, The Netherlands
Giovanni Lancioni, Italy
Jaroslaw Latalski, Poland
Hervé Laurent, France
Agostino Lauria, Italy
Aimé Lay-Ekuakille, Italy
Nicolas J. Leconte, France
Kun-Chou Lee, Taiwan
Dimitri Lefebvre, France
Eric Lefevre, France
Marek Lefik, Poland
Yaguo Lei, China
Kauko Leiviskä, Finland
Ervin Lenzi, Brazil
ChenFeng Li, China
Jian Li, USA
Jun Li, China
Yueyang Li, China
Zhao Li, China
Zhen Li, China
En-Qiang Lin, USA
Jian Lin, China
Qibin Lin, China
Yao-Jin Lin, China
Zhiyun Lin, China
Bin Liu, China
Bo Liu, China
Heng Liu, China
Jianxu Liu, Thailand
Lei Liu, China
Sixin Liu, China
Wanquan Liu, China
Yu Liu, China
Yuanchang Liu, United Kingdom
Bonifacio Llamazares, Spain
Alessandro Lo Schiavo, Italy
Jean Jacques Loiseau, France
Francesco Lolli, Italy
Paolo Lonetti, Italy
António M. Lopes, Portugal
Sebastian López, Spain
Luis M. López-Ochoa, Spain
Vassilios C. Loukopoulos, Greece
Gabriele Maria Lozito, Italy
Zhiguo Luo, China
Gabriel Luque, Spain
Valentin Lychagin, Norway
YUE MEI, China
Junwei Ma, China
Xuanlong Ma, China
Antonio Madeo, Italy
Alessandro Magnani, Belgium
Toqeer Mahmood, Pakistan
Fazal M. Mahomed, South Africa
Arunava Majumder, India
Sarfraz Nawaz Malik, Pakistan
Paolo Manfredi, Italy
Adnan Maqsood, Pakistan
Muazzam Maqsood, Pakistan
Giuseppe Carlo Marano, Italy
Damijan Markovic, France
Filipe J. Marques, Portugal
Luca Martinelli, Italy
Denizar Cruz Martins, Brazil

Francisco J. Martos, Spain
Elio Masciari, Italy
Paolo Massioni, France
Alessandro Mauro, Italy
Jonathan Mayo-Maldonado, Mexico
Pier Luigi Mazzeo, Italy
Laura Mazzola, Italy
Driss Mehdi, France
Zahid Mehmood, Pakistan
Roderick Melnik, Canada
Xiangyu Meng, USA
Jose Merodio, Spain
Alessio Merola, Italy
Mahmoud Mesbah, Iran
Luciano Mescia, Italy
Laurent Mevel, France
Constantine Michailides, Cyprus
Mariusz Michta, Poland
Prankul Middha, Norway
Aki Mikkola, Finland
Giovanni Minafò, Italy
Edmondo Minisci, United Kingdom
Hiroyuki Mino, Japan
Dimitrios Mitsotakis, New Zealand
Ardashir Mohammadzadeh, Iran
Francisco J. Montáns, Spain
Francesco Montefusco, Italy
Gisele Mophou, France
Rafael Morales, Spain
Marco Morandini, Italy
Javier Moreno-Valenzuela, Mexico
Simone Morganti, Italy
Caroline Mota, Brazil
Aziz Moukrim, France
Shen Mouquan, China
Dimitris Mourtzis, Greece
Emiliano Mucchi, Italy
Taseer Muhammad, Saudi Arabia
Ghulam Muhiuddin, Saudi Arabia
Amitava Mukherjee, India
Josefa Mula, Spain
Jose J. Muñoz, Spain
Giuseppe Muscolino, Italy
Marco Mussetta, Italy
Hariharan Muthusamy, India
Alessandro Naddeo, Italy
Raj Nandkeolyar, India
Keivan Navaie, United Kingdom
Soumya Nayak, India
Adrian Neagu, USA
Erivelton Geraldo Nepomuceno, Brazil
AMA Neves, Portugal
Ha Quang Thinh Ngo, Vietnam
Nhon Nguyen-Thanh, Singapore
Papakostas Nikolaos, Ireland
Jelena Nikolic, Serbia
Tatsushi Nishi, Japan
Shanzhou Niu, China
Ben T. Nohara, Japan
Mohammed Nouari, France
Mustapha Nourelfath, Canada
Kazem Nouri, Iran
Ciro Núñez-Gutiérrez, Mexico
Wlodzimierz Ogryczak, Poland
Roger Ohayon, France
Krzysztof Okarma, Poland
Mitsuhiro Okayasu, Japan
Murat Olgun, Turkey
Diego Oliva, Mexico
Alberto Olivares, Spain
Enrique Onieva, Spain
Calogero Orlando, Italy
Susana Ortega-Cisneros, Mexico
Sergio Ortobelli, Italy
Naohisa Otsuka, Japan
Sid Ahmed Ould Ahmed Mahmoud, Saudi Arabia
Taoreed Owolabi, Nigeria
EUGENIA PETROPOULOU, Greece
Arturo Pagano, Italy
Madhumangal Pal, India
Pasquale Palumbo, Italy
Dragan Pamučar, Serbia
Weifeng Pan, China
Chandan Pandey, India
Rui Pang, United Kingdom
Jürgen Pannek, Germany
Elena Panteley, France
Achille Paolone, Italy

George A. Papakostas, Greece
Xosé M. Pardo, Spain
You-Jin Park, Taiwan
Manuel Pastor, Spain
Pubudu N. Pathirana, Australia
Surajit Kumar Paul, India
Luis Payá, Spain
Igor Pažanin, Croatia
Libor Pekař, Czech Republic
Francesco Pellicano, Italy
Marcello Pellicciari, Italy
Jian Peng, China
Mingshu Peng, China
Xiang Peng, China
Xindong Peng, China
Yuexing Peng, China
Marzio Pennisi, Italy
Maria Patrizia Pera, Italy
Matjaz Perc, Slovenia
A. M. Bastos Pereira, Portugal
Wesley Peres, Brazil
F. Javier Pérez-Pinal, Mexico
Michele Perrella, Italy
Francesco Pesavento, Italy
Francesco Petrini, Italy
Hoang Vu Phan, Republic of Korea
Lukasz Pieczonka, Poland
Dario Piga, Switzerland
Marco Pizzarelli, Italy
Javier Plaza, Spain
Goutam Pohit, India
Dragan Poljak, Croatia
Jorge Pomares, Spain
Hiram Ponce, Mexico
Sébastien Poncet, Canada
Volodymyr Ponomaryov, Mexico
Jean-Christophe Ponsart, France
Mauro Pontani, Italy
Sivakumar Poruran, India
Francesc Pozo, Spain
Aditya Rio Prabowo, Indonesia
Anchasa Pramuanjaroenkij, Thailand
Leonardo Primavera, Italy
B Rajanarayan Prusty, India
Krzysztof Puszynski, Poland
Chuan Qin, China
Dongdong Qin, China
Jianlong Qiu, China
Giuseppe Quaranta, Italy
DR. RITU RAJ, India
Vitomir Racic, Italy
Carlo Rainieri, Italy
Kumbakonam Ramamani Rajagopal, USA
Ali Ramazani, USA
Angel Manuel Ramos, Spain
Higinio Ramos, Spain
Muhammad Afzal Rana, Pakistan
Muhammad Rashid, Saudi Arabia
Manoj Rastogi, India
Alessandro Rasulo, Italy
S.S. Ravindran, USA
Abdolrahman Razani, Iran
Alessandro Reali, Italy
Jose A. Reinoso, Spain
Oscar Reinoso, Spain
Haijun Ren, China
Carlo Renno, Italy
Fabrizio Renno, Italy
Shahram Rezapour, Iran
Ricardo Riaza, Spain
Francesco Riganti-Fulginei, Italy
Gerasimos Rigatos, Greece
Francesco Ripamonti, Italy
Jorge Rivera, Mexico
Eugenio Roanes-Lozano, Spain
Ana Maria A. C. Rocha, Portugal
Luigi Rodino, Italy
Francisco Rodríguez, Spain
Rosana Rodríguez López, Spain
Francisco Rossomando, Argentina
Jose de Jesus Rubio, Mexico
Weiguo Rui, China
Rubén Ruiz, Spain
Ivan D. Rukhlenko, Australia
Dr. Eswaramoorthi S., India
Weichao SHI, United Kingdom
Chaman Lal Sabharwal, USA
Andrés Sáez, Spain

Bekir Sahin, Turkey
Laxminarayan Sahoo, India
John S. Sakellariou, Greece
Michael Sakellariou, Greece
Salvatore Salamone, USA
Jose Vicente Salcedo, Spain
Alejandro Salcido, Mexico
Alejandro Salcido, Mexico
Nunzio Salerno, Italy
Rohit Salgotra, India
Miguel A. Salido, Spain
Sinan Salih, Iraq
Alessandro Salvini, Italy
Abdus Samad, India
Sovan Samanta, India
Nikolaos Samaras, Greece
Ramon Sancibrian, Spain
Giuseppe Sanfilippo, Italy
Omar-Jacobo Santos, Mexico
J Santos-Reyes, Mexico
José A. Sanz-Herrera, Spain
Musavarah Sarwar, Pakistan
Shahzad Sarwar, Saudi Arabia
Marcelo A. Savi, Brazil
Andrey V. Savkin, Australia
Tadeusz Sawik, Poland
Roberta Sburlati, Italy
Gustavo Scaglia, Argentina
Thomas Schuster, Germany
Hamid M. Sedighi, Iran
Mijanur Rahaman Seikh, India
Tapan Senapati, China
Lotfi Senhadji, France
Junwon Seo, USA
Michele Serpilli, Italy
Silvestar Šesnić, Croatia
Gerardo Severino, Italy
Ruben Sevilla, United Kingdom
Stefano Sfarra, Italy
Dr. Ismail Shah, Pakistan
Leonid Shaikhet, Israel
Vimal Shanmuganathan, India
Prayas Sharma, India
Bo Shen, Germany
Hang Shen, China
Xin Pu Shen, China
Dimitri O. Shepelsky, Ukraine
Jian Shi, China
Amin Shokrollahi, Australia
Suzanne M. Shontz, USA
Babak Shotorban, USA
Zhan Shu, Canada
Angelo Sifaleras, Greece
Nuno Simões, Portugal
Mehakpreet Singh, Ireland
Piyush Pratap Singh, India
Rajiv Singh, India
Seralathan Sivamani, India
S. Sivasankaran, Malaysia
Christos H. Skiadas, Greece
Konstantina Skouri, Greece
Neale R. Smith, Mexico
Bogdan Smolka, Poland
Delfim Soares Jr., Brazil
Alba Sofi, Italy
Francesco Soldovieri, Italy
Raffaele Solimene, Italy
Yang Song, Norway
Jussi Sopanen, Finland
Marco Spadini, Italy
Paolo Spagnolo, Italy
Ruben Specogna, Italy
Vasilios Spitas, Greece
Ivanka Stamova, USA
Rafał Stanisławski, Poland
Miladin Stefanović, Serbia
Salvatore Strano, Italy
Yakov Strelniker, Israel
Kangkang Sun, China
Qiuqin Sun, China
Shuaishuai Sun, Australia
Yanchao Sun, China
Zong-Yao Sun, China
Kumarasamy Suresh, India
Sergey A. Suslov, Australia
D.L. Suthar, Ethiopia
D.L. Suthar, Ethiopia
Andrzej Swierniak, Poland
Andras Szekrenyes, Hungary
Kumar K. Tamma, USA

Yong (Aaron) Tan, United Kingdom
Marco Antonio Taneco-Hernández, Mexico
Lu Tang, China
Tianyou Tao, China
Hafez Tari, USA
Alessandro Tasora, Italy
Sergio Teggi, Italy
Adriana del Carmen Téllez-Anguiano, Mexico
Ana C. Teodoro, Portugal
Efstathios E. Theotokoglou, Greece
Jing-Feng Tian, China
Alexander Timokha, Norway
Stefania Tomasiello, Italy
Gisella Tomasini, Italy
Isabella Torcicollo, Italy
Francesco Tornabene, Italy
Mariano Torrisi, Italy
Thang nguyen Trung, Vietnam
George Tsiatas, Greece
Le Anh Tuan, Vietnam
Nerio Tullini, Italy
Emilio Turco, Italy
Ilhan Tuzcu, USA
Efstratios Tzirtzilakis, Greece
FRANCISCO UREÑA, Spain
Filippo Ubertini, Italy
Mohammad Uddin, Australia
Mohammad Safi Ullah, Bangladesh
Serdar Ulubeyli, Turkey
Mati Ur Rahman, Pakistan
Panayiotis Vafeas, Greece
Giuseppe Vairo, Italy
Jesus Valdez-Resendiz, Mexico
Eusebio Valero, Spain
Stefano Valvano, Italy
Carlos-Renato Vázquez, Mexico
Martin Velasco Villa, Mexico
Franck J. Vernerey, USA
Georgios Veronis, USA
Vincenzo Vespri, Italy
Renato Vidoni, Italy
Venkatesh Vijayaraghavan, Australia
Anna Vila, Spain
Francisco R. Villatoro, Spain
Francesca Vipiana, Italy
Stanislav Vítek, Czech Republic
Jan Vorel, Czech Republic
Michael Vynnycky, Sweden
Mohammad W. Alomari, Jordan
Roman Wan-Wendner, Austria
Bingchang Wang, China
C. H. Wang, Taiwan
Dagang Wang, China
Guoqiang Wang, China
Huaiyu Wang, China
Hui Wang, China
J.G. Wang, China
Ji Wang, China
Kang-Jia Wang, China
Lei Wang, China
Qiang Wang, China
Qingling Wang, China
Weiwei Wang, China
Xinyu Wang, China
Yong Wang, China
Yung-Chung Wang, Taiwan
Zhenbo Wang, USA
Zhibo Wang, China
Waldemar T. Wójcik, Poland
Chi Wu, Australia
Qiuhong Wu, China
Yuqiang Wu, China
Zhibin Wu, China
Zhizheng Wu, China
Michalis Xenos, Greece
Hao Xiao, China
Xiao Ping Xie, China
Qingzheng Xu, China
Binghan Xue, China
Yi Xue, China
Joseph J. Yame, France
Chuanliang Yan, China
Xinggang Yan, United Kingdom
Hongtai Yang, China
Jixiang Yang, China
Mijia Yang, USA
Ray-Yeng Yang, Taiwan

Contents

Hindawi
Mathematical Problems in Engineering
Volume 2022, Article ID 7436749, 16 pages
https://doi.org/10.1155/2022/7436749

Research Article

Sustainability Assessment of Electricity Generation Development under the Implementation of Support Policies with Endogenous Financial Resources Using a Hybrid Decision Support Model

Fateme Dianat,[1] Vahid Khodakarami ,[1] Hamed Shakouri Ganjavi,[2,3] and Seyed-Hossein Hosseini[4]

[1]*Industrial Engineering Department, Faculty of Engineering, Bu-Ali Sina University, Hamedan, Iran*
[2]*School of Industrial and Systems Engineering, College of Engineering, University of Tehran, Tehran, Iran*
[3]*NuGrid Power Corp., Vancouver, BC, Canada*
[4]*Model-based Management Systems Institute (SAMAM), Tehran, Iran*

Correspondence should be addressed to Vahid Khodakarami; v.khodakarami@basu.ac.ir

Received 19 January 2022; Accepted 28 April 2022; Published 18 May 2022

Academic Editor: Reza Maihami

Sustainable electricity development is one of the requirements for achieving sustainable development in global communities. However, due to barriers, especially in less developed countries, there is little incentive to invest in the development of sustainable electricity technologies. Therefore, there should be a change in market mechanisms, and broad support policies have to be implemented for the sustainable development of electricity. In the long run, these policies must lead to the sustainable development of energy systems. To evaluate the efficiency and effects of the proposed support policies on the sustainability of electricity generation development, this study intends to analyze the multiple and complex dimensions of the problem using a hybrid decision support model. Moreover, by defining an indicator to assess the electricity generation expansion sustainability, this study assists policymakers in making logical decisions about sustainable support programs for the electricity development based on the characteristics of the electricity market of each country. Despite uncertainties in the electricity market, simulations show that the results of this hybrid model have approximately 88% conformance with historical data. Consequently, the model can evaluate the sustainability of the system under the implementation of the proposed support programs and compare them to select the most effective one. The results show that by assuming a competitive market and rational behavior and implementing support programs with endogenous financial resources, the installed renewable capacity can be improved by up to 70.4% compared with the direct subsidy policies. Regardless of the financial burden of policies (e.g., direct subsidies) and the possibility of facing a budget deficit, these programs can be up to 79.2% more effective in the sustainability of the energy system compared with the direct subsidy policy.

1. Introduction

Sustainable development of electricity generation, which is a vital part of sustainable development, is achieved when its generation and consumption provide development in all economic, social, environmental, technical, and institutional aspects of human life in the long run [1, 2].

The energy efficiency, required land, water and fuel consumption, Operation and Maintenance (O&M) costs, initial investment costs, number of jobs created, the amount of electricity generated, and the volume of greenhouse gases produced are some parameters in the evaluation of the sustainability of an electricity generation technology [2, 3].

Numerous studies have shown that renewable electricity technologies are highly compliant with sustainability criteria and are deemed sustainable energy sources [4, 5].

However, due to several reasons, especially in less developed countries, such as inadequate infrastructures, unreliable laws to support the development of renewable electricity generation, absence of pollution tariffs, high initial investment expenses for renewable power plants, and cheap fossil fuel (especially in countries rich in fossil resources), the construction of fossil power plants is still economically profitable [3]. Accordingly, there is low motivation in such countries to invest in developing renewable electricity technologies. As a result, governments need to pave the way for the development of renewable electricity by changing the market mechanisms or introducing support programs [6].

Plans like tax cuts and technical subsidies for renewable energy development [7], feed-in tariffs (FIT) [7–10], fuel price reforming [10], tradable green certification (TGC) market [7, 11], and carbon emission tax [10, 12, 13] are instances of such support plans.

In selecting appropriate support programs to achieve sustainable development, given the high initial investment costs of constructing a new renewable power plant capacity, it cannot be simply assumed that production is carried out at a constant rate [8]. In studies such as [14], the amount of funding needed for decision-makers to achieve specific goals under different scenarios is analyzed, while issues such as how they are funded, the effects of their scarcity, and the prediction of the financial crises are not considered. For long-term development, in addition to considering the system's variables such as supply, demand, and pricing as endogenous, one should also think about financing new capacities and implementing these support programs [15]. If a decision-maker does not plan for covering these costs (e.g., as stated in [8]), the implementation of support plans (such as the FIT policy) with no feedback from the financial resources leads to the failure of the development plan despite the temporary satisfactory development effects. Plus, by causing a budget deficit for the government [16], they bring no profit except for short-term and unsustainable growth.

Sustainability in energy systems has recently attracted the attention of researchers, and extensive literature exists on this topic. Table 1 summarizes some key characteristics of recent studies on sustainable energy systems.

The present study attempts to evaluate support programs and their impacts on the development of electricity by identifying the dynamics and influential factors in renewable and conventional electricity development using a decision support model that matches the complexity of the problem. This article defines a comprehensive criterion using which the sustainability of electricity generation development can be properly measured and quantitatively compared under different support programs.

A comprehensive and precise decision support model is proposed, which simulates the trend of system variables under different scenarios with decent accuracy. This model can be highly reliable for creating a macro perspective of the entire electricity generation system of a country since it takes into account the competition between players, the interaction between variables, and the uncertainties in the system. With the help of simulations executed on the hybrid model, decision-makers can observe the effects of the proposed support programs on the system before implementation and select the most sustainable support policies for the development of electricity generation with the least financial burden for the government.

The remainder of this study is as follows. In Section 2, the research method is stated. Section 3 presents a criterion for the sustainability of the support programs, the conceptual model of the problem, and the method of modeling the competition between renewable electricity technologies and conventional electricity generation technologies. In Section 4, the validity of the model is evaluated. In the next step, by assuming that these programs are implemented, their effects on the sustainability of the electricity generation development and the installed capacity of renewable power plants are measured in Section 5. Finally, Section 6 concludes the article.

2. Methodology

Achieving sustainability goals in planning the development of power generation technologies requires a comprehensive analysis of the complexities of the electricity market. Therefore, this research begins by using qualitative methods such as interviewing experts in the electricity industry and studying previous research to identify the problem and its main influential factors. To assess the performance and make the right decision about the formulation of appropriate support programs that lead to the sustainable development of electricity generation, it is necessary to use a decision support model that addresses important aspects of the system, including the dynamics of problem variables, feedback relationships, and the interactions of players in a competitive market and an uncertain environment. In this research, the combination of the system dynamics (SD) simulation and the concepts of agent-based modeling (ABM) is used as a suitable decision support model for analysis. In this way, SD is used to model the complex structure of influential continuous variables, while ABM concepts are used to model the interaction between players, such as the competition between renewable power plants and other conventional ones.

Liberalized electricity markets include several heterogeneous generators that compete based on their type of technology and risk-taking capacity. As a result, such markets deal with different agents (electricity generators) that form a multiagent (multiplayer) problem. However, due to the limited number of participants, the electricity market model is generally similar to an oligopoly (imperfect competition).

To simplify modeling, the problem was solved for two players: (1) wind power generators (which represent renewable power plants because of their maturity and abundance [30]) and (2) combined-cycle gas turbines (CCGT, generators that represent conventional power plants since they offer high efficiency among fossil fuel generators and countries show more tendency toward their construction). By assuming a competitive market, the evolutionary game theory (EGT) method was used to find the equilibrium point of the game. Iran's electricity market data [31] (as a sample to inspect the effects of the selected plans) were employed to perform this modeling for the period from 2010

Table 1: Recent studies on sustainable energy systems.

Aim of the study	Year	Methodology	Energy case study	Support program	With endogenous financial resources	Dimension of sustainability				
						Environmental	Economic	Social	Technical	Institutional
Evaluation of the effect of subsidies for the construction of Home Solar Power Plants (HSPPs) on sustainable energy systems [14]	2022	System Dynamics (SD)	HSPPs	Subsidy		*	*	*	*	*
A comparative study of FIT and Renewable Portfolio Standard (RPS) policy [17]	2015	Optimization	Renewable and nonrenewable electricity	FIT and RPS	*	*	*	*	*	
Evaluation of renewable energy development [18]	2013	SD	Renewable energy			*	*		*	
Evaluation of renewable energy policy [19]	2015	SD	Renewable and nonrenewable electricity			*	*	*		*
Creation of a model for the assessment of the sustainable development of energy systems [20]	2017	Multicriteria decision analysis (MCDA)	Energy systems (all forms of energy)	Subsidy		*	*	*		
Assessment of the dynamics of FIT policy [8]	2020	SD	Renewable energy	FIT	*		*	*	*	*
Feasibility study of switching the electrical power supply [21]	2017	Engineering economics	Solar photovoltaic (PV) and nonrenewable electricity	Electricity tariffs		*	*		*	
Sustainability analysis of PV/wind/diesel hybrid energy systems for decentralized energy generation [22]	2020	Optimization	PV/wind/diesel/battery (hybrid energy)			*	*	*	*	*
Sustainable energy planning in Africa [23]	2020	Multicriteria decision analysis (MCDA)	Renewable energy			*	*	*	*	
The role of geothermal resources in sustainable power system planning [24]	2020	SD	Geothermal electricity			*	*		*	
The impact of the under enforcement of RPS in China [25]	2019	SD	Renewable and nonrenewable electricity	RPS	*		*			*
Multicriteria optimization for the design and operation of distributed energy systems [26]	2021	Optimization	Distributed energy systems			*	*	*		

Table 1: Continued.

Aim of the study	Year	Methodology	Energy case study	Support program	With endogenous financial resources	Dimension of sustainability				
						Environmental	Economic	Social	Technical	Institutional
Reduction in carbon dioxide emissions [10]	2022	SD	Renewable and nonrenewable electricity	FIT, carbon cost, eliminating fossil fuel power plant's subsidies		*	*	*	*	*
Simulating the new British Electricity-Market Reform [27]	2015	SD	Renewable and nonrenewable electricity	FIT, carbon price, capacity mechanism		*	*		*	*
Environmental and economic performance of China's Emissions Trading Scheme (ETS) pilots [28]	2021	Scenario and regression analysis	Industrial sector (i.e., mining, manufacturing, producing and supplying electricity, heat, gas, and water)	ETS	*	*	*			
Analysis of renewable energy subsidy in China under uncertainty [16]	2021	Optimization	Renewable and nonrenewable electricity	FIT and RPS	*	*	*	*	*	
Confronting electricity challenges [29]	2019	SD	Renewable and nonrenewable electricity	Energy efficiency measures, Electric Vehicle (EV) expansion, and renewables policies		*	*	*	*	*
This study	2022	SD and Agent-Based Modeling (ABM) concepts	Renewable and nonrenewable electricity	Direct subsidy and support programs with endogenous financial resource	*	*	*	*	*	*

to 2050. Moreover, the historical data from 2010 to 2019 were compared with the model behavior to validate the modeling. After ensuring the accuracy of the model, assuming the existence of a rational behavior between players and a competitive market, support programs with endogenous financial resources (that are assumed to be functional after 2022) were executed in the model so that they can be compared, and their effects on the system and their efficiency can be analyzed.

3. Model

To resolve concerns about the possibility of the termination of support programs due to financial pressures on governments [15] and budget deficiencies resulting from the implementation of programs such as FIT [8, 16], this study assumes that support programs with endogenous financial resources are sustainable, and evaluates their sustainability. Assuming a rational relationship between price changes and supply and demand, along with a competitive market, and inspired by a variety of support policies implemented in the world [7, 30], this study evaluates the sustainability of the three following support policies and offers solutions to provide implementation costs:

(i) Support policy 1 (SP1): taxing the emission of pollutants and allocating its revenue to wind power systems as subsidies

(ii) Support policy 2 (SP2): modifying the fuel price and allocating its revenue to wind power systems as subsidies

(iii) Support policy 3 (SP3): taxing electricity consumers and allocating the obtained revenue to wind power systems as subsidies

These support plans increase profitability and appeal of investment in the development of their capacity by subsidizing the generation of renewable electricity per kilowatt-hour (kWh), which increases its generation. Figure 1 shows the influence mechanisms of the mentioned support programs on the development of renewable electricity capacity.

Each support policy affects various aspects of the power generation system upon implementation, such as the amount of pollutant gas emissions or the development rate of renewable electricity generation. However, the effectiveness of implementing a support policy cannot be assessed solely based on the increase in the installed capacity of a power plant. In particular, implementing a policy may increase the price of electricity or the unemployment rate in other electricity generation technologies, which are not in line with the interests of consumers. Therefore, decision-makers should carefully evaluate the effects of support programs from various aspects. In this regard, a criterion should be defined that provides a quick macro view of the effects of implementing support programs on electricity generation development for better policy-making decisions.

Several studies [32, 33] have assessed the sustainability of energy systems under the influence of different electricity generation technologies using various methods such as multiple-criteria decision-making (MCDM) [34]. Based on the focus of each study, performance indicators and various parameters have been proposed to evaluate the sustainability of an energy system, as listed in a review study [1]. In general, the sustainability of energy systems can be examined in five aspects: economic, social, environmental, technical, and institutional [2]. Using the parameters introduced in studies such as [1, 3], the present study proposes a criterion to determine the sustainability of the electricity generation expansion, called the electricity development sustainability index (EDSI), to provide a comprehensive view of the effectiveness of each support program. To achieve research objectives, after receiving comments from electricity industry experts, and taking into account model boundary and regardless of the implementation cost of support programs, the following factors are considered to affect EDSI:

Competitiveness of renewable electricity and its market share [35, 36]

Net job creation of the electricity industry [3, 36]

Greenhouse gas emissions [36, 37]

Consumer demand coverage [3, 23]

Price affordability [1]

As shown in Figure 2, EDSI improves with the growth in the share of renewable electricity in electricity generation and its competitiveness in the market. This index also increases with the creation of jobs in the electricity industry (i.e., the total number of jobs created in the renewable and nonrenewable electricity industry) and the coverage of consumer demand. Finally, generating electricity at a reasonable and affordable price and reducing greenhouse gases are other influential factors.

EDSI is normalized based on the first year of the study (2010), and as a result, its value for this year is one. This index is a relative quantity that can be used to understand the expansion trend of the electricity generation system toward sustainability or unsustainability, compare the proposed support programs, and provide policymakers with a better view, assisting their decisions.

To simulate the EDSI and understand how it is affected by the implementation of support programs, it is necessary to simulate the involved factors. As shown in Figure 1, one of the most significant factors affecting the tendency toward new investments in different generation technologies is the investor's expected profitability ratio (IEPR), which depends on income and the levelized cost of energy (LCOE), as shown in the following equation:

$$\mathrm{IEPR} = \frac{\mathrm{Income} - \mathrm{LCOE}}{\mathrm{LCOE}}. \tag{1}$$

The tendency toward new investment has been studied in the literature under titles such as Willingness For Investment (WFI) [9] or the attractiveness of constructing new power plants [10], which depends on its IEPR, and the IEPR of other power plants.

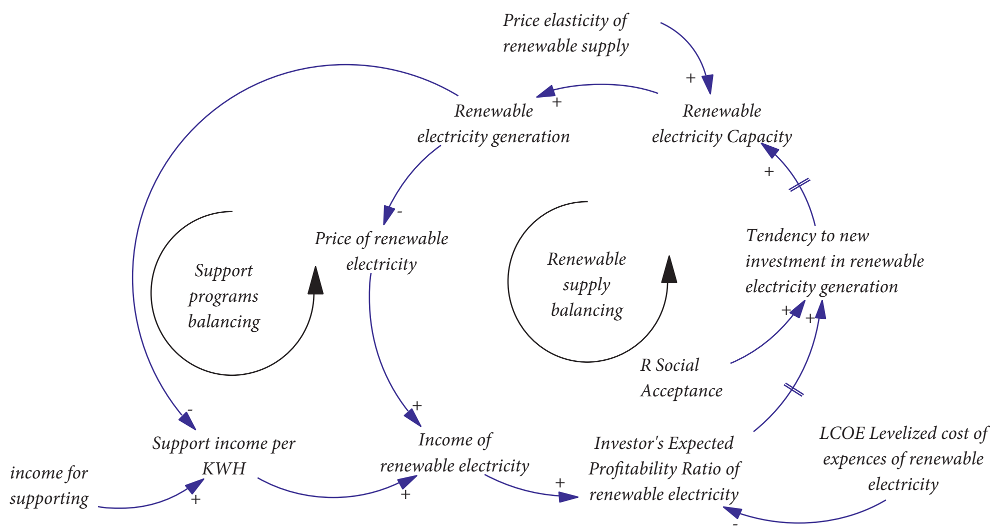

Figure 1: The effect of support programs on increasing the profitability of renewable electricity generation.

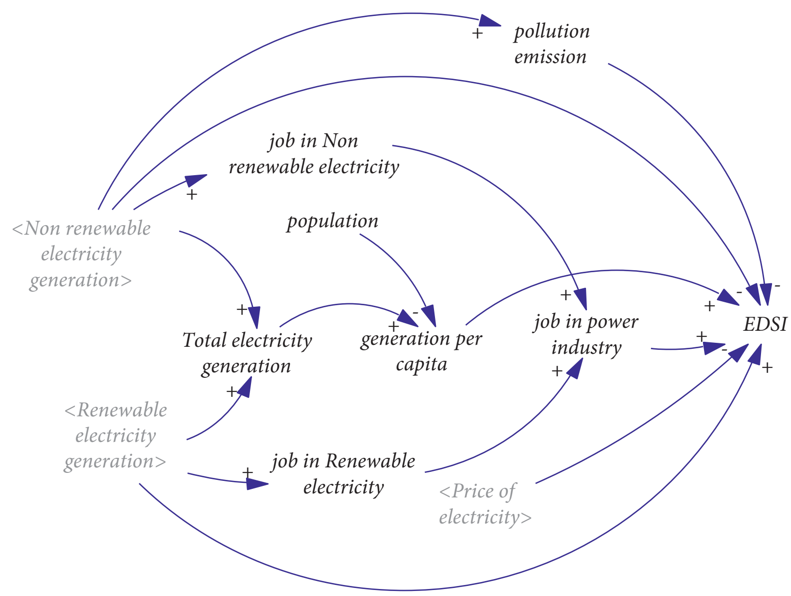

Figure 2: The relationship between the factors affecting EDSI.

It is evident that price, as the outcome of the interaction and balance between supply and demand in a competitive environment, plays a significant role in calculating IEPR and the tendency toward new investment.

The price of electricity is partially related to the price elasticity of supply and demand. In other words, increasing the generation in power plants yields lower electricity prices, which means higher profit due to quantity and lower profit due to price. In contrast, if power plants generate less electricity, insufficient delivery of electricity increases the price, which means higher profit regarding price and lower profit regarding quantity.

However, price is also affected by the competition mechanism of power plants in the electricity market. To elaborate, each power plant needs to adjust its behavior (price and generation capacity) based on the behavior of other power plants (i.e., they need to offer a competitive price for their electricity in accordance with the price of their competitors). Optimal bidding in the electricity market increases the profit of power plants. In order to have a more extensive view and accurate evaluation, we need to analyze factors that affect the market, including the dynamics of the development of renewable and nonrenewable power plants. Since the goal is to inspect the long-term trend of the system under support programs, and the long-term behavior of the market usually occurs in its stable equilibrium points, this study seeks to find the equilibrium bidding point in the electricity market.

The relationships between price, supply, and demand in a competitive market are shown in Figure 3. In this figure, endogenous funded support programs are marked with red arrows.

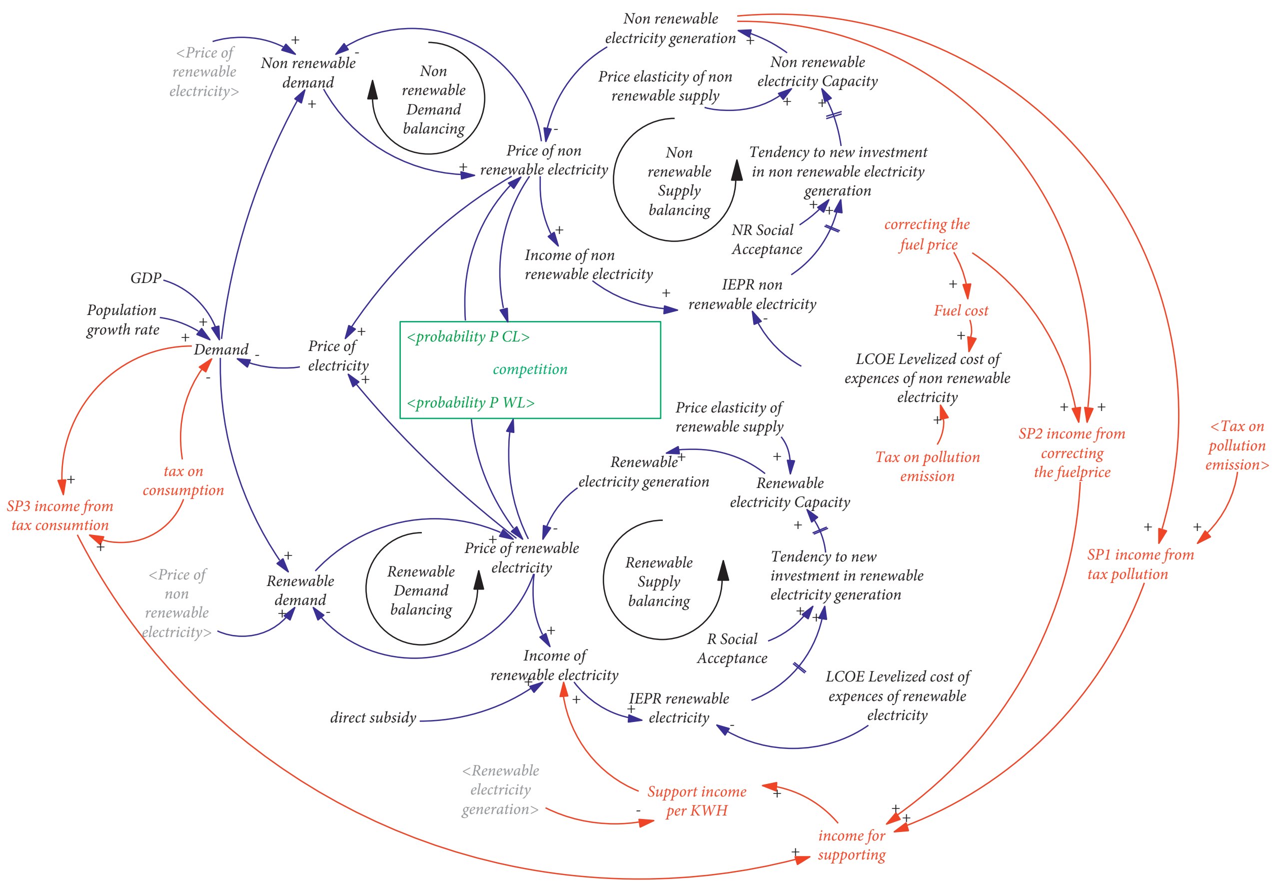

Figure 3: The relationships between price, supply, and demand in support plans with endogenous financial resources.

For competition analysis, game theory-based models are used as decision support tools, which are mainly used for the analysis of oligopoly competitions. According to the game theory, the ultimate price for market players occurs in the Nash equilibrium of market competition, where no player is willing to change its strategy to increase its profit.

3.1. Finding the Equilibrium Point of the Games. By reviewing the literature on game theory [38–43], it can be concluded that the methods for finding the Nash equilibrium points in competitive and noncooperative games can be divided into four categories based on the mathematical equations of the system and finiteness or infiniteness of the proposed pricing options, as shown in Figure 4.

In this figure, competition results of categories 1 and 3 are strongly influenced by the format of the objective function and relationships between variables [40]. However, in the real world, a different number of participants and decision variables can compete in the market with specific delays, sequential and feedback relationships, uncertainties, conditional relationships, and linear and nonlinear relationships with other participants. Moreover, different scenarios can be explored. As a result, objective functions become dependent on several factors, which makes the modeling of the problem as mathematical equations a time-consuming and challenging task. Furthermore, oligopoly market models, which rely only on the equation-based game theory, usually suffer from three shortcomings: disregarding feedback loops, disregarding time delays, and being limited to the definitive demand function [40]. This research studies the electricity market, which has high levels of intrinsic complexity and uncertainty sources with several feedback relations. Hence, solutions 1 and 3 are not appropriate for finding equilibrium points in this competition.

Since the bidding price is a continuous variable, price options are infinite. Therefore, solution 2 is not accurate in finding an equilibrium price. Thus, to apply more realistic conditions and inspect the effects of different scenarios on electricity development sustainability in the uncertain and competitive environment of the electricity market, it is more appropriate to use the fourth category [42, 43]: the evolutionary strategy solution (i.e., the gradual finding of the answer).

Studies comparing the results of game equilibrium using different methods [41] showed that if Nash equilibrium exists and the game assumptions are realistic, all solution methods converge to the same results [44, 45].

Solutions provided in categories 1, 2, and 3 in Figure 4 can only find the final equilibrium point, while they offer no information about the system's path to the final solution. On the other hand, the evolutionary strategy solution, in addition to converging to the equilibrium point,

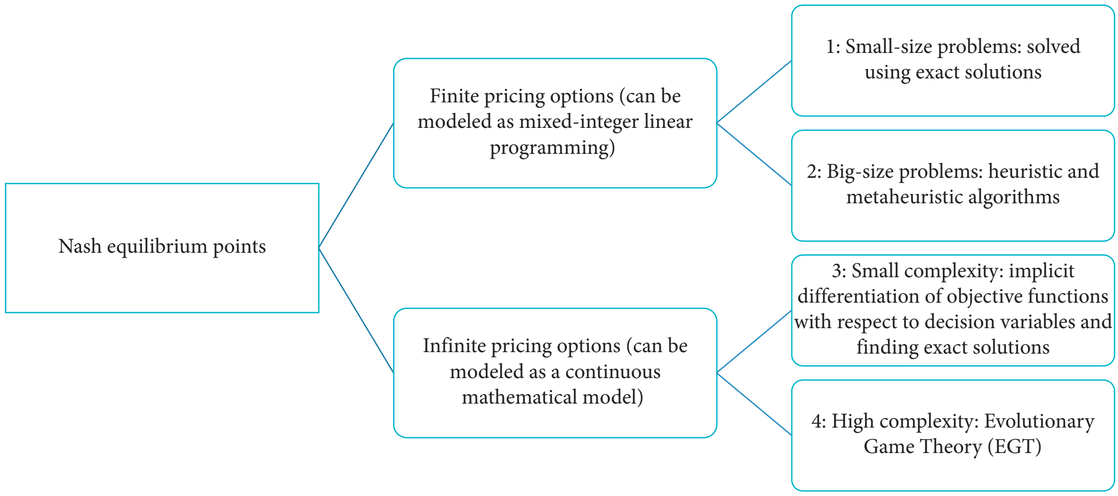

Figure 4: Categories of solutions for finding the equilibrium point of the games.

gives the decision-maker information about how players dynamically decide in reaching the equilibrium point [42, 46].

3.2. Competition Modeling. The model assumes that the "pay as bid pricing" is the payment mechanism for market clearing price (MCP). To motivate investment in the construction of new power plants and the development of generation, each power plant should try to achieve more revenue and less cost (higher IEPR), compared to other competitors, according to the power generation and price bidding of the market. In this way, their tendency to invest in capacity expansion also increases.

The adopted strategy and the profit of each player affect the profit of other competitors. Their decision to determine the price or quantity of their generated electricity results from an oligopoly game. At the equilibrium point, where all players consider each other's strategies, their IEPRs are maximized. The model determines the acceptable quantity and price for the generation of power plants so that while they continue generation, the development of power plants can also be achieved simultaneously.

In the evolutionary strategy solution, a probability of selecting or disregarding a strategy is assigned to each player. The value of this probability indicates the willingness of the player to select that strategy. The probability of choosing a behavior depends on its reward.

In modeling the competition between two power plants, P_{WL} is defined as the probability of offering a low price and P_{WH} is the probability of offering a high price by the wind power plants. Similarly, P_{CL} is the probability of offering a low price and P_{CH} is the probability of offering a high price by CCGT. The relation between these parameters is shown in equations (2) and (3)

$$P_{\mathrm{WL}} = 1 - P_{\mathrm{WH}}, \tag{2}$$

$$P_{\mathrm{CL}} = 1 - P_{\mathrm{CH}}. \tag{3}$$

As a result, four pricing conditions are formed. It is necessary to calculate the IEPR of each player in these four pricing conditions to find the equilibrium point and the best strategy for each player.

W_{WLCL} IEPR of the wind power plant when P_{WL} and P_{CL} occur, meaning that both the wind power plant and the CCGT power plant bid a low price.

W_{WLCH} is the IEPR of the wind power plant when P_{WL} and P_{CH} occur, meaning that the wind power plant bids a low price while the CCGT power plant bids a high price.

W_{WHCL} is the IEPR of the wind power plant when P_{WH} and P_{CL} occur, meaning that the wind power plant bids a high price, and the CCGT power plant bids a low price.

W_{WHCH} is the IEPR of the wind power plant when P_{WH} and P_{CH} occur, meaning that both the wind power plant and the CCGT power plant bid a high price.

Moreover, C_{WLCL}, C_{WLCH}, C_{WHCL}, and C_{WHCH} are the corresponding IEPRs of CCGT power plants under similar bidding conditions.

The IEPR in each bidding condition is determined according to the electricity price levels of the power plant, the electricity price levels of other power plants, and the effect of these prices on the power generation.

The IEPRs of players dynamically and continuously change as the output of the SD model, and their results are continuously fed into the game model to decide on the equilibrium point (Figure 5).

To solve the game, the values of the variables U_{PWL} (utility of the wind power plant if P_{WL} occurs, regardless of the CCGT's bidding price), U_{PWH} (utility of the wind power plant if P_{WH} occurs, regardless of the CCGT's bidding price), U_{PCL} (utility of the CCGT power plant if P_{CL} occurs, regardless of the wind power plant's bidding price), U_{PCH} (utility of the CCGT power plant if P_{CH} occurs, regardless of the wind power plant's bidding price), $\overline{U}_W$ (the average utility of the wind power plant, under any bidding price condition), and $\overline{U}_C$ (the average utility of the CCGT power plant, under any bidding price condition) are calculated according to equations (4) and (5).

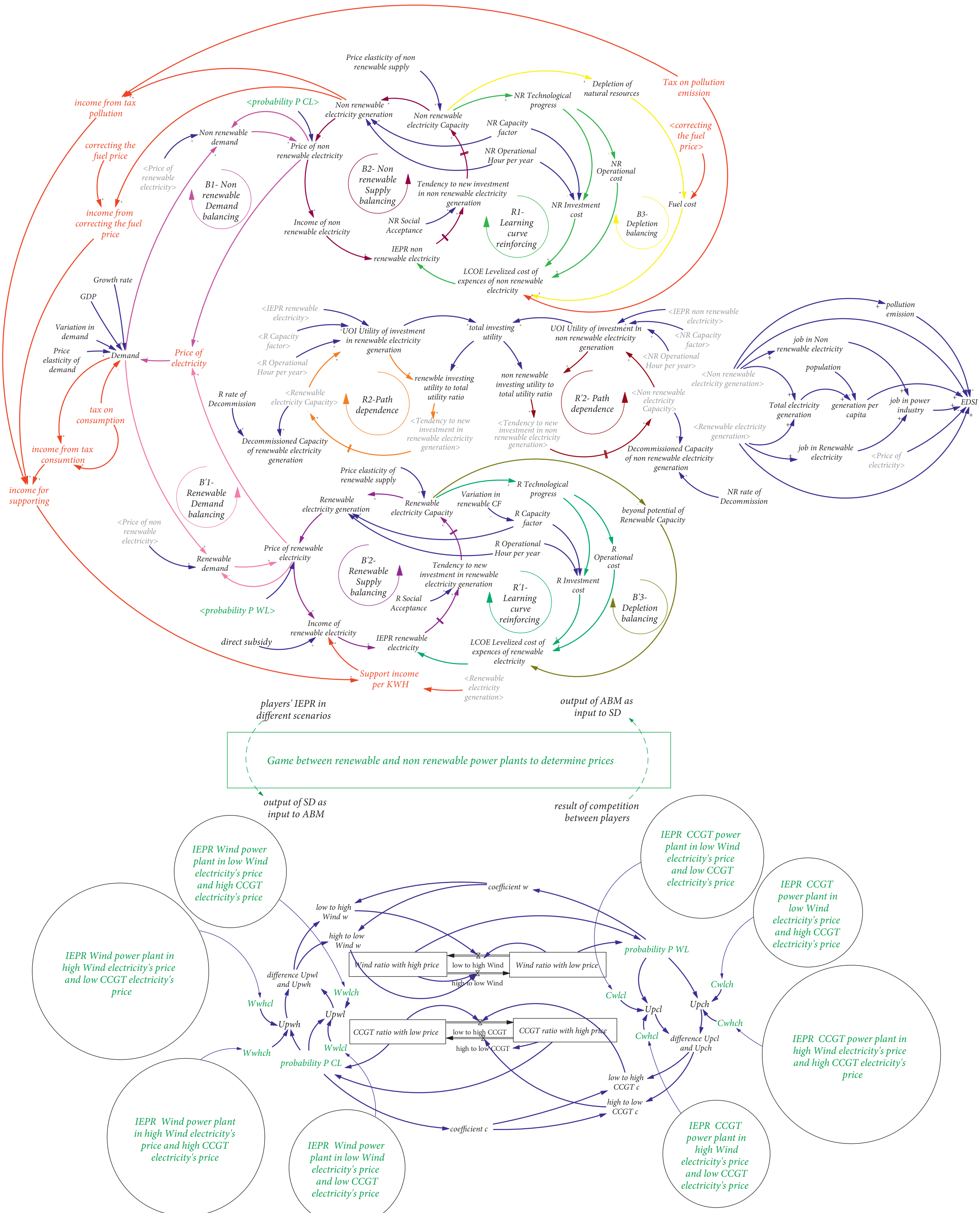

Figure 5: Power market subsystems.

$$\begin{cases} U_{\mathrm{PWL}} = P_{\mathrm{CL}} \times W_{\mathrm{WLCL}} + P_{\mathrm{CH}} \times W_{\mathrm{WLCH}} \\ U_{\mathrm{PWH}} = P_{\mathrm{CL}} \times W_{\mathrm{WHCL}} + P_{\mathrm{CH}} \times W_{\mathrm{WHCH}} \end{cases} \longrightarrow \overline{U}_W = P_{\mathrm{WL}} \times U_{\mathrm{PWL}} + P_{\mathrm{WH}} \times U_{\mathrm{PWH}}, \tag{4}$$

$$\begin{cases} U_{\mathrm{PCL}} = P_{\mathrm{WL}} \times C_{\mathrm{WLCL}} + P_{\mathrm{WH}} \times C_{\mathrm{WHCL}} \\ U_{\mathrm{PCH}} = P_{\mathrm{WL}} \times C_{\mathrm{WLCH}} + P_{\mathrm{WH}} \times C_{\mathrm{WHCH}} \end{cases} \longrightarrow \overline{U}_C = P_{\mathrm{CL}} \times U_{\mathrm{PCL}} + P_{\mathrm{CH}} \times U_{\mathrm{PCH}}. \tag{5}$$

Equilibrium occurs when players are reluctant to change their strategy to gain more utility and maintain their bidding strategy in the market. In other words, according to equations (6) and (7), we have

$$\frac{\mathrm{d}P_{\mathrm{WL}}}{\mathrm{d}t} = P_{\mathrm{WL}} \times \left(U_{\mathrm{PWL}} - \overline{U}_W\right) = P_{\mathrm{WL}} \times P_{\mathrm{WH}} \left(P_{\mathrm{CL}} \times \left(W_{\mathrm{WLCL}} - W_{\mathrm{WHCL}}\right) + P_{\mathrm{CH}} \times \left(W_{\mathrm{WLCH}} - W_{\mathrm{WHCH}}\right)\right) = 0. \tag{6}$$

$$\frac{\mathrm{d}P_{\mathrm{CL}}}{\mathrm{d}t} = P_{\mathrm{CL}} \times \left(U_{\mathrm{PCL}} - \overline{U}_C\right) = P_{\mathrm{CL}} \times P_{\mathrm{CH}} \left(P_{\mathrm{WL}} \times \left(C_{\mathrm{WLCL}} - C_{\mathrm{WLCH}}\right) + P_{\mathrm{WH}} \times \left(C_{\mathrm{WHCL}} - C_{\mathrm{WHCH}}\right)\right) = 0. \tag{7}$$

The points that simultaneously answer the above equations are equilibrium points. These points can be stable or unstable. In order to determine the stability of equilibrium points of the system's replicate dynamic equations, the Friedman condition for the Jacobian matrix [47] or Lyapunov's theory of stability must be satisfied [25, 42]. In our case, since the IEPRs of players continuously change, the unstable equilibrium answer cannot be maintained, and the system converges to the steady equilibrium state.

When a strategy is successful in the evolutionary game, the movement toward it occurs gradually, and eventually, the answers to the evolutionary strategies converge to the Nash equilibrium point [42, 46]. The game equilibrium answer re-enters the SD and changes the model variables. As a result, a two-way relationship is observed between the SD and the game part, and the hybrid decision support model operates in a connected and integrated manner. The conceptual model of the problem ultimately takes the form of Figure 5.

Figure 5 illustrates the following: the relationship between demand and price in balancing loops B1 and B′1 [48], the effect of learning in reinforcing loops R1 and R′1 [8, 49, 50], the relationship between supply and price in balancing loops B2 and B′2 [48], dynamics of path dependence (the concept of the share of each player to the share of other players [40]) in the reinforcing loops R2 and R′2, and the effect of resource depletion in the balancing loops B3 and B′3 [49, 50]. This model can take into account the effects of social acceptance [8, 50], sensitivity analysis for possible uncertainties [51], and competition between electricity market players. By regarding a vast number of variables affecting the system and their interrelations [52], this model can evaluate the effects of several proposed support programs on the sustainability of power generation development and provide the decision-maker with a comprehensive view.

3.3. Data and Mathematical Equations. In this study, Iran's electricity market data (energy balance), published by the Power Ministry of Iran [31], was used for modeling. Additional data were also extracted from statistics published by CCGT and wind power plants and articles that studied Iran's electricity generation [10], including the historical data of wind farms and CCGT capacities, the fuel cost of CCGT power plants, discount rates, fixed and variable O&M costs, and the annual number of jobs created per gigawatt-hour electricity generation using wind power and CCGT. General parameters such as natural gas heat rate and the capacity factor (CF) of CCGT and wind power plants (mentioned in articles such as [53]) were also utilized.

After extracting the necessary data, the mathematical equations of the model and the relationship between model variables were determined using the studies on electricity generation in Iran (e.g., [8, 10, 54]) and interviewing experts in the energy field and employees of the Power Ministry. The data and mathematical equations were developed in the form of stock-flow diagrams in Vensim software using the conceptual model depicted in Figure 5.

It was assumed that, according to Table 2, a tax would be levied on CCGT power plants in proportion to the pollutant emissions to implement the SP1, which changes the LCOE of CCGT power plants.

It was also assumed that implementing SP2 would increase the fuel cost for Iran's CCGT power plants from \$0.3 to \$0.9 per MMBtu, consequently changing the LCOE of CCGT power plants similar to SP1. In addition, it was assumed that consumers should pay an additional \$0.003 per kWh electricity consumption as tax to implement the SP3. The modeling also simulates the direct subsidy relative to underdevelopment (DSRU) program.

The DSRU program is an instance of the FIT policy for renewable electricity. DSRU has also been mentioned in some articles as a policy of closeness to the goal [8], a policy in which renewable electricity power plants receive less support as renewable energy share increases. The DSRU simulation assumed that wind farms would receive \$0.35 per kWh generated electricity until they reach 1% of the market share and \$0.21 per kWh generated electricity until they reach 5% of the market share.

Table 2: Emission cost and emission factor.

Pollution	NO_X	SO_2	CO	PM	CO_2	CH_4
Emission cost ($/g)	0.00107278	0.00326289	0.000335222	0.00768789	0.0000178889	0.000374222
Emission factor (g/MMBtu)	200	25	1	9	60000	1.5

4. Verification and Validation

Before using the model to analyze support programs, its validity was investigated using several tests to ensure the accuracy of the results. Specifically, to verify the framework (boundary adequacy and structure assessment), the reasonableness of the dynamics of renewable and nonrenewable electricity development trends, balancing and reinforcing loops, and cause-and-effect relationships between the problem variables (Figure 5) were evaluated and approved by renewable electricity experts.

As shown in Figure 6, in 2019, the sustainability of power generation development using the index defined in this study (EDSI) is 2.5 times the historical data from the initial year (2010), indicating that Iran's electricity industry is moving toward sustainable development.

The mean absolute percentage error (MAPE) value was used to evaluate the conformance of the simulated values with the historical data. This rate is 12.1% for EDSI, 0.8% for the demand, 14.6% for wind power capacity, and 3.7% for CCGT power capacity. The Pearson correlation coefficient (a coefficient between 1 and −1) was employed to calculate the correlation between the simulated values and historical data. The obtained values for this coefficient were 0.956 for EDSI, 0.996 for demand, 0.959 for wind power capacity, and 0.976 for CCGT power capacity. Competitive modeling validity and Nash equilibrium were also assessed using the sample data.

5. Results and Discussion

The designed model can determine EDSI over time and under the influence of different support programs. Assuming that there exists a competitive market and that rational behavior prevails, the results of the EDSI under the three support programs (i.e., SP1, SP2, and SP3) are illustrated in diagrams 1, 2, and 3 in Figure 7, respectively. Moreover, the EDSI for the DSRU program is illustrated in diagram 4. Finally, EDSI in the absence of support programs (while it is assumed that the market is competitive and logical behavior prevails) is presented in diagram 5 in Figure 7.

Figure 7 shows that SP1, SP2, and SP3 positively impact the sustainability of power generation development. Although diagram 4 is simulated regardless of the DSRU program implementation cost, the efficiency of the DSRU policy in the sustainability of the energy generation development is still less than the other three mentioned programs that are financed endogenously.

Compared with the absence of support programs, the sustainability of energy generation development was improved by 85.8%, 31.4%, and 13.5% for SP1, SP2, and SP3, respectively. However, the DSRU program could only increase the sustainability of electricity generation development by 3.7% compared with the state of having no support plans.

The capacity development results for CCGT power plants and wind farms are illustrated in Figures 8(a) and 8(b), in respective order, under different scenarios.

As shown by the red arrows in Figure 3, corrections in fuel prices or emission taxes increase the cost of generating conventional electricity, resulting in a lower profit and incentive to invest in the sector. By spending the mentioned revenues on subsidizing renewable electricity generation, the income and profitability of renewable power plants will increase, yielding the development of renewable electricity (Diagrams 1 and 2 of Figure 8). It is evident that these effects intensify as the revenues increase [12].

It is worth mentioning that implementing the tradable green certificate (TGC) market can be considered the opposite of the emission trading system (ETS). While emission trading imposes a cost on nonrenewable electricity generation, TGC generates additional revenue for renewable electricity and ensures that a certain percentage of the electricity generation comes from renewable sources [11]. Therefore, it seems that the implementation of the TGC market, such as taxing the emission of pollutants and allocating its revenue as a subsidy (SP1) or modifying the fuel price and allocating its revenue as a subsidy to wind power systems (SP2), can lead to further development of wind power systems.

Nevertheless, upon the implementation of TGC, a market is created to purchase and sell these certificates, and it seems that the bureaucracy for implementing this program is higher than the two other programs (SP1 and SP2). Due to this bureaucracy, its implementation seems unlikely in countries with a weaker information flow system. This lack of extensiveness may be one of the reasons why TGC markets are utilized mostly in European countries and some US states.

In contrast to SP1 and SP2, which imposed financial pressure on the electricity generated through fossil fuels, SP3 increases the tax paid by consumers for electricity. In the early years of its implementation, consumers may be less willingly involved with this program. As a result, electricity demand in the consumer sector will decrease. However, sensitivity analysis shows that this drop in demand is relatively small and negligible. With the total demand remaining approximately constant, the taxes collected from consumers can be allocated to multiple objectives, including subsidizing per kWh of renewable electricity (diagram 3, Figure 8), offering discounts for initial investments in the construction of wind power plants, or increasing the guaranteed purchase price of the wind power generators. In all cases, positive effects can be seen on the development of renewable electricity capacity and the sustainability of electricity generation development.

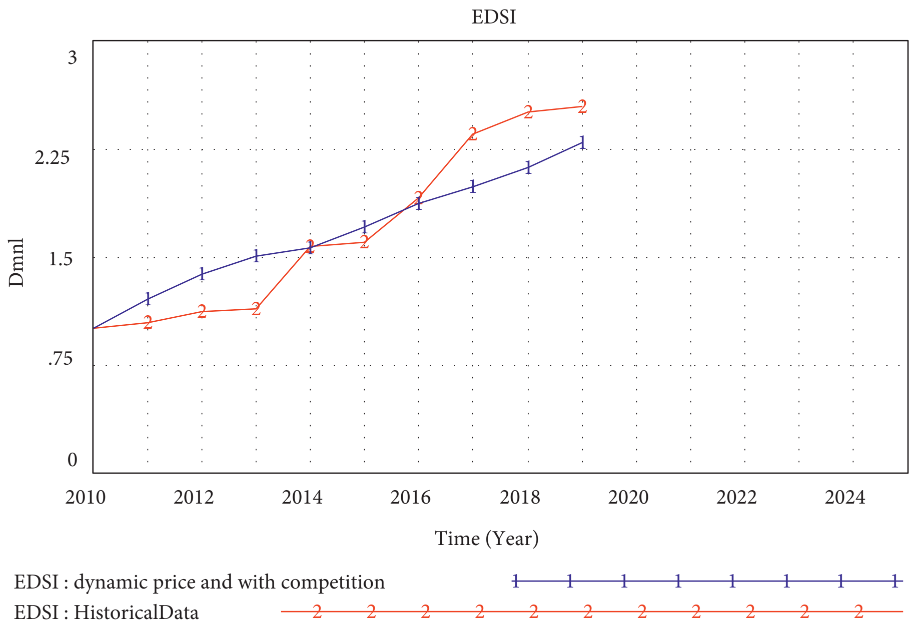

Figure 6: The simulated and historical data for EDSI.

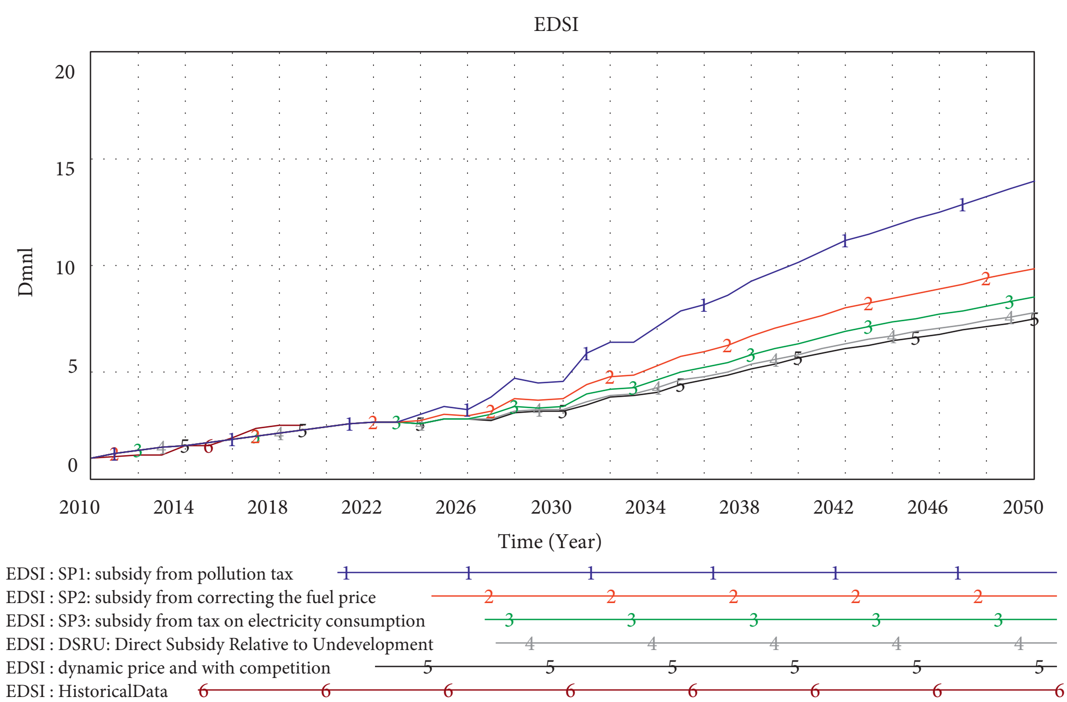

Figure 7: EDSI under different scenarios.

In policies that impose financial pressure on the electricity generated from fossil fuels (SP1 and SP2), revenues are proportional to the electricity generation by CCGT power plants. From another perspective, the incomes obtained from conventional power plants are divided by the capacity of wind power generation to obtain a subsidy per kWh for wind power generation (Figure 1). However, as the generation of wind farms has an upward trend, the amount of subsidy given per kWh of wind power generation decreases (as shown in Figure 9). Simulation results show that although the per kWh subsidies are initially higher than DSRU, they decrease significantly over time. Even though DSRU will be greater than subsidies of SP1, SP2, and SP3 in later years (even if the financial resources of the country are large enough that the budget deficit caused by the DSRU program does not prevent it from continuing), the efficiency of this policy (and the development of wind power as its result) is

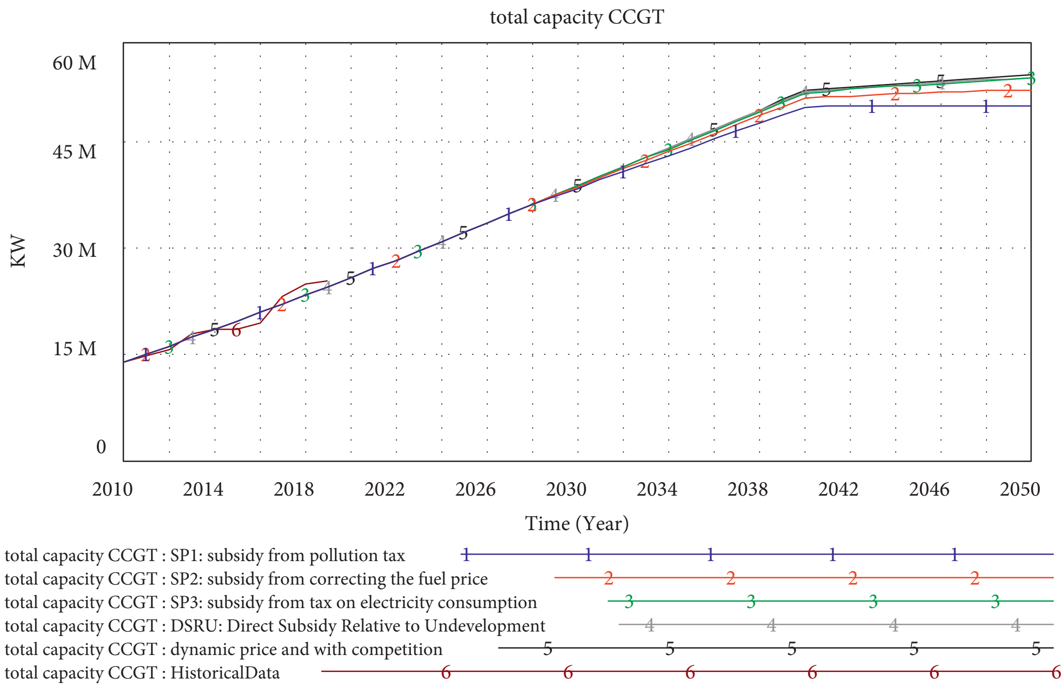

(a)

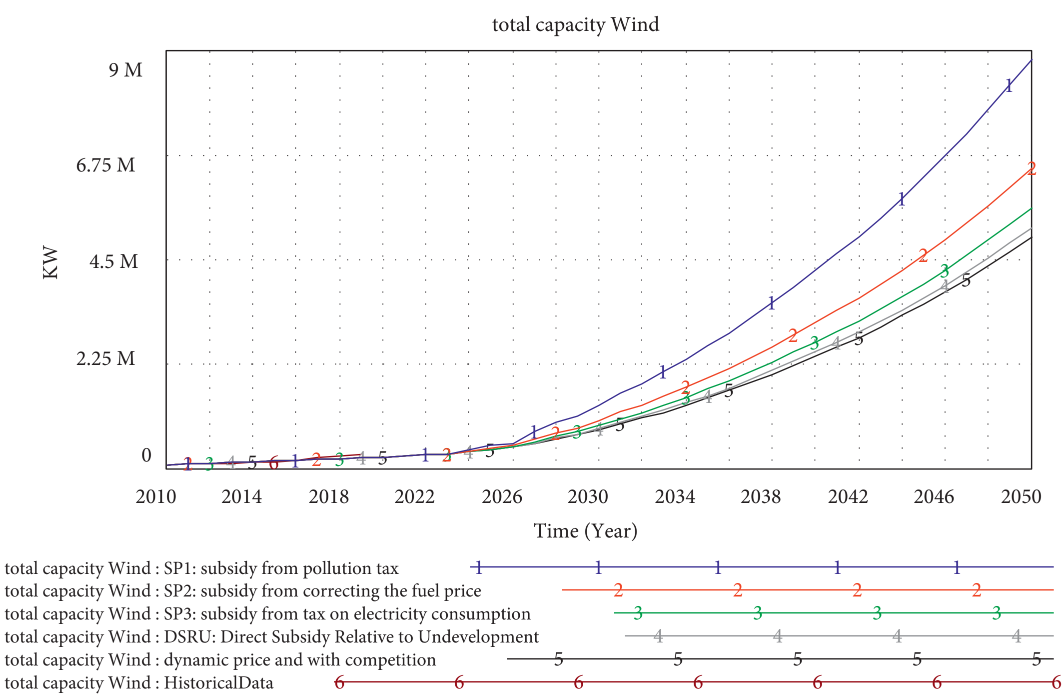

(b)

Figure 8: The installed capacity of CCGT (a) and wind (b) power plants.

less than the rate of development caused by the support policies with endogenous financial resources.

According to Figure 8(b), implementing tax programs on emissions and providing subsidies for wind power (SP1), reforming fuel prices and providing subsidies for wind power (SP2), and taxing consumption and providing subsidies to wind power (SP3) yield an increase of 70.4%, 24.9%, and 8.5% on the installed capacity of wind farms compared with the DSRU program, respectively.

Figure 9, and its correlation to Figure 8(b), shows that appropriate timing for the utilization of incentives, their intensity, and the manner through which these support policies are initiated determine further development of renewable electricity. Midttun and Gautesen [6] also share a similar view.

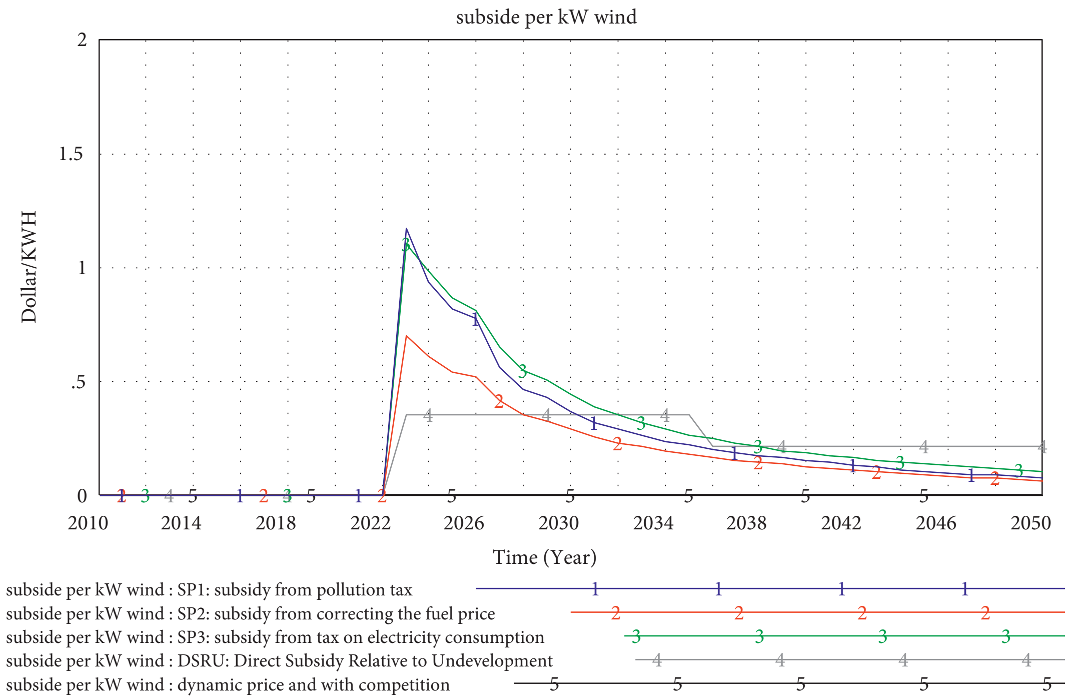

Figure 9: Subsidy per kWh of electricity generated from the wind under different scenarios.

The increased growth rate of any technology reduces its production costs in later stages, which yields further development of power plant capacity and sustainability improvement.

As shown in diagrams 1 and 3 of Figure 9, if it is assumed that the subsidy allocated to wind power, which results from the implementation of taxing programs on emissions (SP1) or consumers (SP3) are equal, SP1 will impose financial pressures on the electricity generated from fossil fuels, reducing the share of this sector in the market (diagrams 1 and 3 of Figure 8(a)). Consequently, by implementing SP1, the capacity of wind farms and EDSI will be 57.1% and 63.6% more than those obtained from implementing SP3, as shown in diagrams 1 and 3 of Figure 8(b) and diagrams 1 and 3 of Figure 7, respectively.

In diagrams 2 and 3 of Figure 9, even though the subsidy given to wind power plants from the fuel price modification program (SP2) is less than that obtained from taxing electricity consumers (SP3) per kWh of wind power generation, the financial pressure on fossil fuel electricity and its effect on reducing the share of this sector in the market (diagrams 2 and 3 Figure 8(a)) increase the capacity of wind farms (diagrams 2 and 3 Figure 8(b)) by 15.1%, and causes EDSI to grow by 15.8% (diagrams 2 and 3 of Figure 7) compared with SP3.

Therefore, implementing financial support programs that impose pressures on fossil fuel electricity (SP1 and SP2) will cause less development in this sector compared with the development caused by subsidies through taxing consumers (SP3) and the DSRU mode (Figure 8(a)). Consequently, if the decision-makers aim to achieve sustainability in the energy generation system, reduce the share of fossil fuel electricity, increase the share of renewable electricity, and reduce emissions, financing policies through pressure on fossil fuel electricity are suggested to be more efficient.

On the other hand, if decision-makers solely aim to increase the total generation capacity of their country's power plants to cover consumer demand, it seems appropriate to tax the total electricity consumption (SP3) as it would not change demand remarkably and would not impose high social costs on governments. However, this practice will not massively influence fossil fuel power plants. In this case, SP3 is suitable for developing both renewable and nonrenewable electricity. Nevertheless, as this scenario generates less clean electricity and more emissions than SP1 and SP2, it has less effect on the sustainability of the energy system.

6. Conclusions

In this study, a hybrid model was used to investigate the effects of support programs on the sustainability of an energy system and the capacity development of renewable power plants. The goal was to provide simultaneous analysis of the main aspects of the problem, including dynamics between factors, feedback relationships, competitiveness, and the uncertain environment of the electricity market. The model was executed using Iran's electricity industry data.

The results show that programs funded from within the system (such as the three programs mentioned in this article) can be considered sustainable support programs for the development of renewable electricity. These programs improve the installed capacity of the wind farms by 8.5% to 70.4% more than direct subsidy policies and do not impose additional costs and financial burdens on the government, while at the same time, they have 9.5% to 79.2% greater development sustainability compared with direct subsidy.

This research has some limitations which can be improved in the future. For example, the demand in the electricity industry can be increased or decreased by imports and exports, depending on the conditions of each country. In this study, the effect of the electricity import and export subsystem has been omitted in the model since Iran's net import and export is negligible in relation to the country's total electricity demand. In future studies, this subsystem can be implemented in the model, particularly for countries with higher electricity imports and exports.

In future research, the sustainability of electricity generation development can also be assessed by implementing other programs (or a combination of programs) that support the development of clean electricity using the proposed model.

Data Availability

The data that support the findings of this study are available from the corresponding author upon reasonable request.

Conflicts of Interest

The authors declare that they have no conflicts of interest.

References

[1] M. Martín-Gamboa, D. Iribarren, D. García-Gusano, and J. Dufour, "A review of life-cycle approaches coupled with data envelopment analysis within multi-criteria decision analysis for sustainability assessment of energy systems," *Journal of Cleaner Production*, vol. 150, pp. 164–174, 2017.

[2] B. Mainali and S. Silveira, "Using a sustainability index to assess energy technologies for rural electrification," *Renewable and Sustainable Energy Reviews*, vol. 41, pp. 1351–1365, 2015.

[3] H. G. Shakouri and S. Aliakbarisani, "At what valuation of sustainability can we abandon fossil fuels? A comprehensive multistage decision support model for electricity planning," *Energy*, vol. 107, pp. 60–77, 2016.

[4] I. Dincer and C. Acar, "A review on clean energy solutions for better sustainability," *International Journal of Energy Research*, vol. 39, no. 5, pp. 585–606, 2015.

[5] S. Hossain, H. Chowdhury, T. Chowdhury et al., "Energy, exergy and sustainability analyses of Bangladesh's power generation sector," *Energy Reports*, vol. 6, pp. 868–878, 2020.

[6] A. Midttun and K. Gautesen, "Feed in or certificates, competition or complementarity? Combining a static efficiency and a dynamic innovation perspective on the greening of the energy industry," *Energy Policy*, vol. 35, no. 3, pp. 1419–1422, 2007.

[7] J. Arias-Gaviria, S. X. Carvajal-Quintero, and S. Arango-Aramburo, "Understanding dynamics and policy for renewable energy diffusion in Colombia," *Renewable Energy*, vol. 139, pp. 1111–1119, 2019.

[8] H. Milad Mousavian, G. Hamed Shakouri, A.-N. Mashayekhi, and A. Kazemi, "Does the short-term boost of renewable energies guarantee their stable long-term growth? Assessment of the dynamics of feed-in tariff policy," *Renewable Energy*, vol. 159, pp. 1252–1268, 2020.

[9] M. S. Shahmohammadi, R. M. Yusuff, S. Keyhanian, G. H. Shakouri, and H. Shakouri, "A decision support system for evaluating effects of Feed-in Tariff mechanism: dynamic modeling of Malaysia's electricity generation mix," *Applied Energy*, vol. 146, pp. 217–229, 2015.

[10] A. Mostafaeipour, A. Bidokhti, M.-B. Fakhrzad, A. Sadegheih, and Y. Zare Mehrjerdi, "A new model for the use of renewable electricity to reduce carbon dioxide emissions," *Energy*, vol. 238, Article ID 121602, 2022.

[11] M. Hasani-Marzooni and S. H. Hosseini, "Dynamic interactions of TGC and electricity markets to promote wind capacity investment," *IEEE Systems Journal*, vol. 6, no. 1, pp. 46–57, 2012.

[12] M. Petitet, D. Finon, and T. Janssen, "Carbon price instead of support schemes: wind power investments by the electricity market," *Energy Journal*, vol. 37, no. 4, pp. 109–140, 2016.

[13] P.-y. Nie, C. Wang, and H.-X. Wen, "Optimal tax selection under monopoly: emission tax vs carbon tax," *Environmental Science and Pollution Research*, vol. 29, no. 8, pp. 12157–12163, 2022.

[14] M. Eftekhari Shahabad, A. Mostafaeipour, H. Hosseini Nasab, A. Sadegheih, and H. Ao Xuan, "A new model to investigate effects of subsidies for home solar power systems using system dynamics approach: a case study," *Sustainable Energy Technologies and Assessments*, vol. 49, Article ID 101706, 2022.

[15] I. Khan, "Sustainable energy infrastructure planning framework: transition to a sustainable electricity generation system in Bangladesh," *Energy and Environmental Security in Developing Countries*, pp. 173–198, 2021.

[16] D.-x. Yang, Y.-q. Jing, C. Wang, P.-y. Nie, and P. Sun, "Analysis of renewable energy subsidy in China under uncertainty: feed-in tariff vs. renewable portfolio standard," *Energy Strategy Reviews*, vol. 34, Article ID 100628, 2021.

[17] P. Sun and P.-y. Nie, "A comparative study of feed-in tariff and renewable portfolio standard policy in renewable energy industry," *Renewable Energy*, vol. 74, pp. 255–262, 2015.

[18] A. Aslani, P. Helo, and M. Naaranoja, "Evaluation of renewable energy development in power generation in Finland," *Journal of Renewable and Sustainable Energy*, vol. 5, no. 6, Article ID 063132, 2013.

[19] A. Al-Sarihia, M. Contestabileb, and J. A. Chernia, "Renewable energy policy evaluation using a system dynamics approach: the case of Oman," in *Proceedings of the 33rd International Conference of the System Dynamics Society*, Cambridge, MA, USA, June 2015.

[20] A. Sahabmanesh and Y. Saboohi, "Model of sustainable development of energy system, case of Hamedan," *Energy Policy*, vol. 104, pp. 66–79, 2017.

[21] S. S. Rashwan, A. M. Shaaban, and F. Al-Suliman, "A comparative study of a small-scale solar PV power plant in Saudi Arabia," *Renewable and Sustainable Energy Reviews*, vol. 80, pp. 313–318, 2017.

[22] B. E. K. Nsafon, A. B. Owolabi, H. M. Butu, J. W. Roh, D. Suh, and J.-S. Huh, "Optimization and sustainability analysis of PV/wind/diesel hybrid energy system for decentralized energy generation," *Energy Strategy Reviews*, vol. 32, Article ID 100570, 2020.

[23] B. E. K. Nsafon, H. M. Butu, A. B. Owolabi, J. W. Roh, D. Suh, and J.-S. Huh, "Integrating multi-criteria analysis with PDCA cycle for sustainable energy planning in Africa: application to hybrid mini-grid system in Cameroon," *Sustainable Energy Technologies and Assessments*, vol. 37, Article ID 100628, 2020.

[24] N. Spittler, B. Davidsdottir, E. Shafiei, J. Leaver, E. I. Asgeirsson, and H. Stefansson, "The role of geothermal

resources in sustainable power system planning in Iceland," *Renewable Energy*, vol. 153, pp. 1081–1090, 2020.

[25] D. Fang, C. Zhao, and A. N. Kleit, "The impact of the under enforcement of RPS in China: an evolutionary approach," *Energy Policy*, vol. 135, Article ID 111021, 2019.

[26] J. D. Fonseca, J.-M. Commenge, M. Camargo, L. Falk, and I. D. Gil, "Multi-criteria optimization for the design and operation of distributed energy systems considering sustainability dimensions," *Energy*, vol. 214, Article ID 118989, 2021.

[27] C. J. Franco, M. Castaneda, and I. Dyner, "Simulating the new British electricity-market reform," *European Journal of Operational Research*, vol. 245, no. 1, pp. 273–285, 2015.

[28] H.-x. Wen, Z.-r. Chen, and P.-y. Nie, "Environmental and economic performance of China's ETS pilots: new evidence from an expanded synthetic control method," *Energy Reports*, vol. 7, pp. 2999–3010, 2021.

[29] G. J. Matthew, W. J. Nuttall, B. Mestel, and L. S. Dooley, "Low carbon futures: confronting electricity challenges on island systems," *Technological Forecasting and Social Change*, vol. 147, pp. 36–50, 2019.

[30] H. E. Murdock, "Renewables 2019 global status report," 2019, https://www.ren21.net/reports/global-status-report Accessed on.

[31] energy balance of Iran, "Ministry of energy (MOE)," 2017, http://isn.moe.gov.ir/.

[32] K. Suomalainen and B. Sharp, "Electricity sector transformation in New Zealand: a sustainability assessment approach," *Journal of Renewable and Sustainable Energy*, vol. 8, no. 3, Article ID 035902, 2016.

[33] Y. Torul Yürek, M. Bulut, B. Özyörük, and E. Özcan, "Evaluation of the hybrid renewable energy sources using sustainability index under uncertainty," *Sustainable Energy, Grids and Networks*, vol. 28, Article ID 100527, 2021.

[34] I. Khan, "Data and method for assessing the sustainability of electricity generation sectors in the south Asia growth quadrangle," *Data in Brief*, vol. 28, Article ID 104808, 2020.

[35] U. Hernandez-Hurtado and C. Martin-del-Campo, "A development of indicators for the sustainability assessment of the Mexican power system planning," *International Journal of Sustainable Energy Planning and Management*, vol. 32, pp. 95–110, 2021.

[36] A. Buchmayr, E. Verhofstadt, L. Van Ootegem, D. Sanjuan Delmás, G. Thomassen, and J. Dewulf, "The path to sustainable energy supply systems: proposal of an integrative sustainability assessment framework," *Renewable and Sustainable Energy Reviews*, vol. 138, Article ID 110666, 2021.

[37] V. Aryanpur, M. S. Atabaki, M. Marzband, P. Siano, and K. Ghayoumi, "An overview of energy planning in Iran and transition pathways towards sustainable electricity supply sector," *Renewable and Sustainable Energy Reviews*, vol. 112, pp. 58–74, 2019.

[38] S. Soleymani, A. Ranjbar, and A. Shirani, "Strategic bidding of generating units in competitive electricity market with considering their reliability," *International Journal of Electrical Power & Energy Systems*, vol. 30, no. 3, pp. 193–201, 2008.

[39] L. Liu and W. Jia, "A new algorithm to solve the generalized Nash equilibrium problem," *Mathematical Problems in Engineering*, vol. 2020, 2020.

[40] A. Mohammadi and E. Javanmardi, "System dynamics modeling of oligopoly market based on game theory," *International Transaction Journal of Engineering, Management, & Applied Sciences & Technologies*, vol. 10, no. 5, pp. 673–687, 2019.

[41] S. Ghazi, J. Dugdale, and T. Khadir, "A multi-agent based approach for simulating the impact of human behaviours on air pollution," 2019, https://arxiv.org/abs/1904.05429.

[42] K. Li, W. Wang, Y. Zhang, T. Zheng, and J. Guo, "Game modelling and strategy research on the system dynamics–based quadruplicate evolution for high–speed railway operational safety supervision system," *Sustainability*, vol. 11, no. 5, p. 1300, 2019.

[43] Y. Zhenlei and G. Chunxia, "Construction and optimization analysis of network knowledge community based on system dynamics," *Mathematical Problems in Engineering*, vol. 2020, pp. 1–8, 2020.

[44] T. Krause, E. V. Beck, R. Cherkaoui, A. Germond, G. Andersson, and D. Ernst, "A comparison of Nash equilibria analysis and agent-based modelling for power markets," *International Journal of Electrical Power & Energy Systems*, vol. 28, no. 9, pp. 599–607, 2006.

[45] C. P. Roca, J. A. Cuesta, and A. Sánchez, "Evolutionary game theory: temporal and spatial effects beyond replicator dynamics," *Physics of Life Reviews*, vol. 6, no. 4, pp. 208–249, 2009.

[46] L. Busoniu, R. Babuska, and B. De Schutter, "A comprehensive survey of multiagent reinforcement learning," *IEEE Transactions on Systems, Man, and Cybernetics, Part C (Applications and Reviews)*, vol. 38, no. 2, pp. 156–172, 2008.

[47] D. Friedman, "On economic applications of evolutionary game theory," *Journal of Evolutionary Economics*, vol. 8, no. 1, pp. 15–43, 1998.

[48] F. Olsina, "Long-term dynamics of liberalized electricity markets," National University of San Juan Argentina, PhD, Thesis submitted to Department of Postgraduate Studies, Faculty of Engineering, 2008.

[49] S. H. Hosseini, S. F. Ghaderi, and G. H. Shakouri, "An investigation on the main influencing dynamics in renewable energy development: a systems approach," in *Proceedings of the Second Iranian Conference on Renewable Energy and Distributed Generation (ICREDG)*, pp. 92–97, IEEE, Tehran, Iran, March 2012.

[50] S. H. Hosseini, G. H. Shakouri, and F. R. Akhlaghi, "A study on the near future of wind power development in Iran: a system dynamics approach," in *Proceedings of the Second Iranian Conference on Renewable Energy and Distributed Generation (ICREDG)*, pp. 183–188, IEEE, Tehran, Iran, March 2012.

[51] X. Liu and M. Zeng, "Renewable energy investment risk evaluation model based on system dynamics," *Renewable and Sustainable Energy Reviews*, vol. 73, pp. 782–788, 2017.

[52] F. Dianat, V. Khodakarami, S.-H. Hosseini, and H. Shakouri G, "Combining game theory concepts and system dynamics for evaluating renewable electricity development in fossil-fuel-rich countries in the Middle East and North Africa," *Renewable Energy*, vol. 190, pp. 805–821, 2022.

[53] A. Ford, K. Vogstad, and H. Flynn, "Simulating price patterns for tradable green certificates to promote electricity generation from wind," *Energy Policy*, vol. 35, no. 1, pp. 91–111, 2007.

[54] S. Moslem Mousavi, M. Bagheri Ghanbarabadi, and N. Bagheri Moghadam, "The competitiveness of wind power compared to existing methods of electricity generation in Iran," *Energy Policy*, vol. 42, pp. 651–656, 2012.

Hindawi
Mathematical Problems in Engineering
Volume 2022, Article ID 4025831, 14 pages
https://doi.org/10.1155/2022/4025831

Research Article

Unsteady MHD Tangent Hyperbolic Nanofluid Past a Wedge Filled with Gyrotactic Micro-Organism

S. M. Atif,[1] Abdul Hamid Ganie,[2] Ilyas Khan ,[3] and M. Andualem [4]

[1]*Department of Mathematics, Roots School System DHA-1, Islamabad, Pakistan*
[2]*Basic Sciences Department, College of Science and Theoretical Studies, Saudi Electronic University, Abha, Male 61421, Saudi Arabia*
[3]*Department of Mathematics, College of Science Al-Zulfi, Majmaah University, Al-Majmaah, Saudi Arabia*
[4]*Department of Mathematics, Bonga University, Bonga, Ethiopia*

Correspondence should be addressed to Ilyas Khan; i.said@mu.edu.sa and M. Andualem; mulugetaandualem4@gmail.com

Received 28 October 2021; Revised 11 January 2022; Accepted 12 April 2022; Published 12 May 2022

Academic Editor: Mohammadreza Safaei

In this numerical investigation, tangent hyperbolic nanofluid past a wedge-shaped surface filled with gyrotactic micro-organisms has been examined. The simulations have been performed in the presence of Ohmic heating and linear thermal radiation effect. After using similarity transformation to convert modeled PDEs into ODEs, the system of ODEs is tackled with the aid of shooting technique. For the authenticity of the code, the present numerical data have been compared with the already existing results in the literature. The impact of important governing parameters on velocity, concentration, temperature, and motile density distribution is examined graphically. Furthermore, the numerical values of the surface drag, heat transfer rate, mass transfer rate, and motile density number are computed and represented in the tabular form. Our simulations indicate that the Nusselt number is enhanced for the growing values of unsteadiness and the velocity ratio parameters. Moreover, a significant raise in nanofluid velocity is observed as magnetic number gets bigger whereas the temperature profile is depressed. For the above proposed model, it can be concluded that heat and mass can be enhanced by using gyrotactic micro-organism.

1. Introduction

Over the years, the enhancement of the thermal conductivity via nanofluids which upsurge the conductivity of conventional fluids has received considerable attention. In this regard, massive theoretical and experimental work have been done and become the most appealing area of the researchers. A significant enhancement in thermal efficiency of nanofluid due to the presence of nanoparticles as compared with ordinary base fluid was observed by Choi [1] in 1995. Thermal conductivity of nanofluid with copper and aluminium oxide nanoparticles was assessed by Lee et al. [2] and Eastman et al. [3]. Sheikholeslami et al. [4] analyzed the numerical solution of alumina nanofluid with MHD effects in a permeable medium. A major finding was that the average Nusselt number is boosted as the Hartmann number is hiked. Goodarzi et al. [5] studied the heat transfer in the nanofluid with Cu, MWCNT, and Al_2O_3 nanoparticles in a cavity with different aspect ratios and concluded that the heat transfer in the cavity is influenced by fluid circulation caused by natural convection and conductive heat transfer mechanism. By considering variable viscosity and thermal radiation, Mondal et al. [6] discussed the magnetohydrodynamic dusty nanofluid. An augmentation in surface drag was noticed for strengthening parametric values of thermophoresis while a decrement in the Nusselt number was observed in accordance with larger Brownian motion parameter. Khamliche et al. [7] ascertained the enhancement of the thermal conductivity of silver nanoparticles with ethylene glycol as based fluid. Their concluding remark was that the thermal conductivity is enhanced by 23% due to addition of 0.1% volume and temperature of 50°C for the Ag nanowires in ethylene glycol as base fluid. Nisar et al. [8] studied the Eyring Powell nanofluid in peristaltic transport with activation energy and reported that the concentration distribution was declined as the activation energy parameter is upsurged. Ellahi et al. [9] investigated two-phase Newtonian hybrid nanofluid flow with Hafnium Particles and slip effects. One of the key observations was that the velocity profile was declined as the Hartmann number is hiked. In a liquid microlayer inside a microreactor, production of the heat transfer by plasmon was reported by Sarafraz and Christo [10]. They concluded that the strongest phase change occurred at light wavelength of 680 nm. Heat transfer in MHD boundary layer flow past a wedge with viscous effects and porous media was ascertained by Ibrahim and Tulu [11]. Atif et al. [12] studied MHD tangent hyperbolic nanofluid past a wedge. Effects of thermal radiation, internal heat generation, and buoyancy on velocity and heat transfer in the Blasius flow were reported by Ibrahim et al. [13]. One of the main conclusions was that the temperature profile declines as the Grashof number is heightened. For further details, refer [14–23].

The non-Newtonian fluids which are electrically conducting allied with a magnetic field have wide-ranging applications in numerous fields like pharmaceutical and hydrometallurgical industry. This has generated a keen interest among the modern day researchers. MHD is widely used to modify the flow field in the desired directions. MHD tangent hyperbolic fluid flow over a stretching cylinder was reported by Malik et al. [24]. It was noticed that the increment in magnetic parameter upturns the resistance to the fluid flow. Ellahi et al. [25] presented the MHD and slip effects on heat transfer boundary layer flow over a moving plate based on specific entropy generation. Jabeen et al. [26] explored the MHD boundary layer flow caused by nonlinear stretching surface in the presence of the porous medium. It was obtained that the velocity profile on increasing magnetic parameter increases whereas the other two profiles, namely, thermal and concentration show the reverse trends for increasing magnetic parameter. Ramzan et al. [27] ascertained the Hall and Ion slip effects in 3D tangent hyperbolic nanofluid. Gharami et al. [28] explored the MHD unsteady flow using the tangent hyperbolic nanofluid model along with chemical reaction and thermal radiation effects. It was concluded that the Nusselt number and skin friction closer to the wall subsided for the higher values of magnetic and thermophoretic parameters. Effect of zero mass flux conditions on tangent hyperbolic nanofluid was studied by Shafiq et al. [29]. Numerical study of momentum and heat transfer of MHD Carreau nanofluid over exponentially stretched plate with internal heat source/sink and radiation was studied by Yousif et al. [30]. An extensive literature on the flow of the MHD tangent hyperbolic fluid model considering different effects over different geometries can be seen in [31–37].

The motile micro-organisms which are self-propelled are added in order to increase the suspensions stability. These micro-organisms rise the base fluid density in response to additional stimulant. Xu and Cui [38] investigated the mixed convective flow under the slip effects and porous medium containing nanoparticles and micro-organisms and found that the variation in the Reynolds number alters all the quantities of physical interest. Pal and Mondal [39] discussed the effect of nonlinear thermal radiation and chemical reaction on bioconvective MHD nanofluid flow with gyrotactic micro-organisms in an exponential stretching sheet. A major finding was that the nanoparticles concentration is enhanced as the chemical reaction parameter is boosted. Atif et al. [40] studied the MHD micropolar nanofluid with gyrotactic micro-organisms. Linear stability of bioconvection nanofluid was performed by Zhao et al. [41] and noticed that the suspension becomes unstable if the thermal Raleigh number is increased to 1750. Saini and Sharma [42] reported that the intermediate swimmers have destabilizing effect, and for smaller values of the wave number, the subcritical region of instability becomes large. Recently, Al-Khaled et al. [43] explored the nonlinear thermal radiation effects on the flow of the bioconvective tangent hyperbolic nanofluid model with chemical reaction. This study revealed that the rate of heat transfer is enhanced for higher thermophoretic parameter.

In fluid dynamics boundary layer, wedge flow is a classic problem and is presented everywhere in fluid dynamics. It can be seen in manufacturing units, industrial processes, or the design of prototypes for technological advancements in aerospace or defense laboratories. Application of the wedge flow could be found in molten metals flow over a ramped surface nuclear power plants, flow of chilled air through AC panels, designing of flaps on airplane wings for the enhancement of the lift, manoeuvre and drag, modeling of warships, submarines, and in several other domains of science and engineering. In fact, wedge angle plays a crucial role in the study of transonic flows over airfoils and wings, including flows at Mach 1 [44].

On analyzing the all existing reports, it is noticed that no one has studied the non-Newtonian tangent hyperbolic nanofluid in the presence of gyrotactic micro-organism yet. The prime objective of this study is to investigate theoretically, the effect of Ohmic heating, magnetic parameter, and linear thermal radiation on tangent hyperbolic nanofluid flow over a wedge-shaped body filled with gyrotactic micro-organisms. The equations which govern the flow and heat transfer are numerically solved via a numerical technique called shooting method. The variation due to important parameters of physical interest involved in the governing system of equations are studied graphically and discussed in detail. The influence of the important parameters on skin friction, Nusselt number, Sherwood number, and motile density number has been studied and presented in the form of tables. Moreover, for the authenticity of the shooting code, numerical values of the skin friction coefficient which were already reported in the literature have been reproduced.

2. Problem Formulation

Two-dimensional unsteady tangent hyperbolic fluid flow in the presence of nanoparticles past a wedge surface has been analyzed. For the stability of the nanofluid, self-propelled micro-organism is considered. The stretching velocity of the wedge is considered as velocity $U_w(x,t) = bx^m/1 - ct$. The

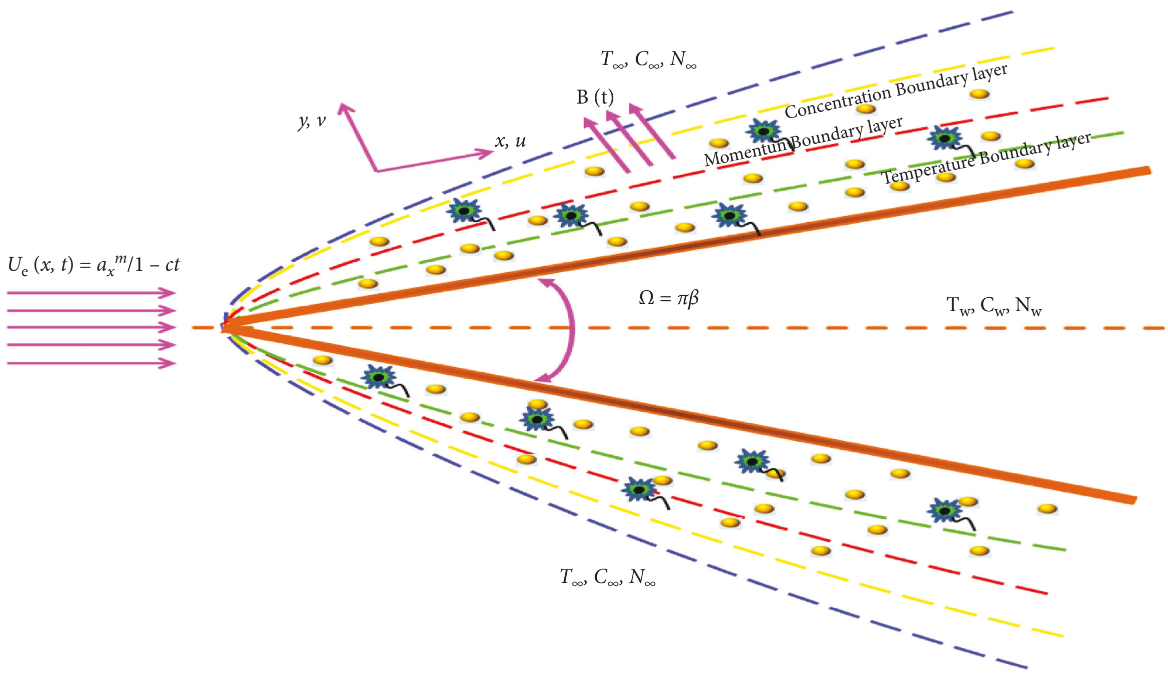

Figure 1: Flow configuration.

nose shaped object is placed along $x-$ axis and $y-$ axis and is perpendicular to the wedge as illustrated in Figure 1. The free stream velocity is assumed as $U_e(x,t) = ax^m/1 - ct$ with $0 \le m \le 1$, and m, a, and c are constants. The surface temperature, surface nanoparticles concentration, and surface micro-organism's concentration are defined as $T_w(x,t) = T_\infty + T_0 U_w x/\nu(1-ct)^{1/2}$, $C_w(x,t) = C_\infty + C_0 U_w x/\nu(1-ct)^{1/2}$, and $N_w(x,t) = N_\infty + N_0 N_w x/\nu(1-ct)^{1/2}$, respectively. Time-dependent magnetic field $B(t) = B_0/(1-ct)^{1/2}$ perpendicular to wedge has also been considered. Induced magnetic field is negligible due to the assumption of the small magnetic Reynolds number.

2.1. Assumptions and Constraints

(1) 2D laminar unsteady flowing
(2) Boundary layer estimation
(3) Non-Newtonian tangent hyperbolic fluid
(4) Ohmic heating
(5) Buongiorno model
(6) Small Reynolds number
(7) Thermal radiative flow

Under the above assumptions, the governing equations of the above modeled problem are as follows [40–50]:

$$\frac{\partial u}{\partial x} + \frac{\partial v}{\partial y} = 0,$$

$$\frac{\partial u}{\partial t} + u\frac{\partial u}{\partial x} + v\frac{\partial u}{\partial y} = \frac{\partial U_e}{\partial t} + U_e\frac{\partial U_e}{\partial x} + \nu\left((1-n) + \sqrt{2}\,n\Gamma\frac{\partial u}{\partial y}\right)\frac{\partial^2 u}{\partial y^2} - \frac{\sigma B_0^2}{\rho}(u - U_e),$$

$$\frac{\partial T}{\partial t} + u\frac{\partial T}{\partial x} + v\frac{\partial T}{\partial y} = \alpha\frac{\partial^2 T}{\partial y^2} - \frac{1}{\rho C_p}\frac{\partial q_r}{\partial y} + \Lambda\left[D_B\frac{\partial C}{\partial y}\frac{\partial T}{\partial y} + \frac{D_T}{T_\infty}\left(\frac{\partial T}{\partial y}\right)^2\right] + \frac{\sigma}{\rho C_p}B_0^2(u - U_e)^2, \quad (1)$$

$$\frac{\partial C}{\partial t} + u\frac{\partial C}{\partial x} + v\frac{\partial C}{\partial y} = \frac{D_T}{T_\infty}\frac{\partial^2 T}{\partial y^2} + D_B\frac{\partial^2 C}{\partial y^2},$$

$$\frac{\partial N}{\partial t} + u\frac{\partial N}{\partial x} + v\frac{\partial N}{\partial y} = D_n\frac{\partial^2 N}{\partial y^2} - \frac{bW_c}{C_w - C_\infty}\left(\frac{\partial N}{\partial y}\frac{\partial C}{\partial y} + N\frac{\partial^2 C}{\partial y^2}\right).$$

The associated BCs are as follows:

$$\left.\begin{array}{l}\text{for } y=0 \;\; u=U_w=\lambda U_e, v=0, T=T_w(x,t), C=C_w(x,t), N=N_w(x,t),\\ \text{as } y\longrightarrow\infty \;\; u\longrightarrow U_e, T\longrightarrow T_\infty, C\longrightarrow C_\infty \;\; N\longrightarrow N_\infty.\end{array}\right\} \quad (2)$$

For the dimensionless equations, the following transformations [45] have been considered:

$$\left.\begin{array}{l}\eta = y\sqrt{\dfrac{(m+1)U_e}{2\nu x}},\\ \psi=\sqrt{\dfrac{2\nu x U_e}{m+1}}f(\eta),\\ \xi(\eta)=\dfrac{N-N_\infty}{N_w-N_\infty},\\ \phi(\eta)=\dfrac{C-C_\infty}{C_w-C_\infty},\\ \theta(\eta)=\dfrac{T-T_\infty}{T_w-T_\infty}.\end{array}\right\}. \quad (3)$$

With the application of the similarity transformation, the continuity equation is automatically satisfied and the transformed ODEs [12, 45, 48–50] are as follows:

$$(1-n+nWef'')f''' -(2-\beta)\left[A\left(\frac{\eta}{2}f''+f'-1\right)+M(f'-1)\right]-\beta\left(f'^2-1\right)+ff''=0, \quad (4)$$

$$\left(1+\frac{4}{3}Rd\right)\theta'' - \Pr\left[(2f'\theta-f\theta')+\frac{A}{2}(2-\beta)(\eta\theta'+3\theta)-Nb\theta'\phi'-Nt\theta'^2-EcM(2-\beta)(f'-1)^2\right]=0, \quad (5)$$

$$\phi''+Sc(f\phi'-2f'\phi)-Sc\frac{A}{2}(2-\beta)(\eta\phi'+3\phi)+\frac{Nt}{Nb}\theta''=0, \quad (6)$$

$$\xi''-Pe(\xi'\phi'+(\xi+\beta^*)\phi'')-Lb[A(2-\beta)(\eta\xi'+3\xi)+(2f'\xi-f\xi')]=0. \quad (7)$$

The BCs after using transformations are

$$\left.\begin{array}{l}\text{for } \eta=0 \;\; f(\eta)=0, f'(\eta)=\lambda, \theta(\eta)=1, \phi(\eta)=1, \xi(\eta)=1\\ \text{as } \eta\longrightarrow\infty \;\; f'(\eta)\longrightarrow 1, \theta(\eta)\longrightarrow 0, \phi(\eta)\longrightarrow 0, \xi(\eta)=0.\end{array}\right\} \quad (8)$$

3. Quantities of Interest

In this section, the dimensional and dimensionless forms of the skin friction, Nusselt, Sherwood, and density numbers are presented.

$$\begin{array}{l}C_f=\dfrac{\tau_w}{\rho u_w^2},\\ Nu_x=\dfrac{xq_w}{k(T_w-T_0)},\\ Sh_x=\dfrac{xq_m}{D_B(C_w-C_0)},\\ Nn_x=\dfrac{xq_n}{D_n(N_w-N_0)}.\end{array} \quad (9)$$

In dimensionless form, these quantities are as follows:

$$\left.\begin{aligned} C_f \mathrm{Re}_x^{1/2}\sqrt{\frac{2}{m+1}} &= \left(1-n+\frac{n}{2}Wef''(0)\right)f''(0),\ Sh_x \mathrm{Re}_x^{-1/2}\sqrt{\frac{2}{m+1}} = -\phi'(0) \\ Nu_x \mathrm{Re}_x^{-1/2}\sqrt{\frac{2}{m+1}} &= -\left(1+\frac{4}{3}Rd\right)\theta'(0).\ Nn_x \mathrm{Re}_x^{-1/2}\sqrt{\frac{2}{m+1}} = -\xi'(0), \end{aligned}\right\} \quad (10)$$

where $Re_x = xU_e/\nu$.

4. Numerical Treatment

4.1. Shooting Technique. The solution of the coupled system of equations (4)–(7) along with BCs equation (8) is achieved with the help of shooting technique.

Now, we introduce new variables $\Psi_1 = f, \Psi_2 = f'$, $\Psi_3 = f''$, $\Psi_4 = \theta$, $\Psi_5 = \theta'$, $\Psi_6 = \phi$, $\Psi_7 = \phi'$, $\Psi_8 = \xi$, and $\Psi_9 = \xi'$.

The system equations and associated boundary conditions are of the form as follows:

$$\left.\begin{aligned} &\Psi_1' = \Psi_2, \\ &\Psi_2' = \Psi_3, \\ &\Psi_3' = \frac{1}{1-n+nWe\Psi_3}\left[(2-\beta)A\left(\frac{\eta}{2}\Psi_3+\Psi_2-1\right)+\beta\left(\Psi_2^2-1\right)-\Psi_1\Psi_3+M(2-\beta)(\Psi_2-1)\right]\Psi_4' = \Psi_5, \\ &\Psi_5' = \frac{-3\mathrm{Pr}}{(3+4Rd)}\left[\Psi_1\Psi_5-2\Psi_2\Psi_4-\frac{A}{2}(2-\beta)(\eta\Psi_5+3\Psi_4)+Nb\,\Psi_5\Psi_7+Nt\,\Psi_5^2+Ec\,M(2-\beta)(\Psi_2-1)^2\right]\Psi_6' = \Psi_7, \\ &\Psi_7' = Sc\left(\frac{A}{2}(2-\beta)(\eta\Psi_7+3\Psi_6)-(\Psi_1\Psi_7-2\Psi_2\Psi_6)\right)-\frac{Nt}{Nb}\Psi_5', \Psi_8' = \Psi_9, \\ &\Psi_9' = Pe\left(\Psi_9\Psi_7+(\Psi_8+\beta^*)\Psi_7'\right)+Lb\left[A(2-\beta)(\eta\Psi_9+3\Psi_8)+2\Psi_2\Psi_6-\Psi_1\Psi_9\right], \end{aligned}\right\} \quad (11)$$

with BCs

$$\left.\begin{aligned} &\text{For } \eta = 0\ \Psi_1(\eta) = 0, \Psi_2(\eta) = \lambda\ \Psi_4(\eta) = 1, \Psi_6(\eta) = 1, \Psi_8(\eta) = 1, \\ &\text{As } \eta \longrightarrow \infty\ \Psi_2(\eta) \longrightarrow 1, \Psi_4(\eta) \longrightarrow 0, \Psi_6(\eta) \longrightarrow 0, \Psi_8(\eta) \longrightarrow 0. \end{aligned}\right\} \quad (12)$$

Unknown initial conditions $\Psi_3(0) = s_1$, $\Psi_5(0) = s_2$, $\Psi_7(0) = s_3$, and $\Psi_9(0) = s_4$ are considered to satisfy the known BCs. Initial guesses s_1, s_2, s_3, and s_4 are refined with the help of Newton's iterative scheme until defined criteria are not achieved. In order to stop the iterative process, following criteria are assumed:

$$\begin{aligned} \max&\left\{\left|\Psi_2(\eta_{\max})-1\right|, \left|\Psi_4(\eta_{\max})-0\right|,\right. \\ &\left.\cdot\left|\Psi_6(\eta_{\max})-0\right|, \left|\Psi_8(\eta_{\max})-0\right|\right\} < 10^{-10}. \end{aligned} \quad (13)$$

We have considered a bounded domain $[0, \infty]$ instead of $[0, \infty)$ for the numerical computations. From our computational experience, it is noticed that boosting $\eta_{\max}$, no substantial fluctuations are noticed in the computational results.

4.2. Flow Chart. Flow chart is shown in Figure 2.

4.3. Code Verification. For the correctness and verification of the MATLAB code, the skin friction values $-f''(0)$ which were reported in the literature by Rajagopal et al. [48], Kuo [49], and Ishak et al. [50] have been reproduced. Our computational results have an admirable agreement with their results (Table 1).

5. Results and Discussion

5.1. The Skin Friction Coefficient. Table 2 is prepared to study the fluctuation in the skin friction coefficient due to the Weissenberg number We, unsteadiness parameter A, velocity ratio parameter λ, power law index n, Hartree pressure gradient β, and magnetic parameter M. Our simulations depict that the skin friction coefficient $Re_x^{-1/2}C_f\sqrt{2/m+1}$ is vitiated for the higher values of velocity ratio parameter λ and power law index n while a hike up is observed for enhancing

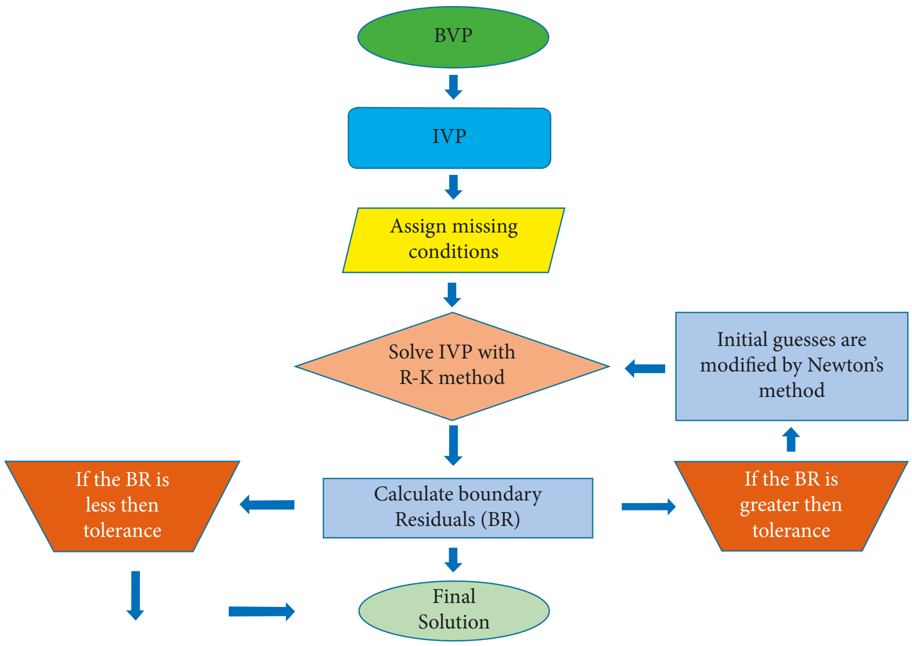

FIGURE 2: Flow chart.

TABLE 1: Numerical data of the computed values of $-f''(0)$ [48–50].

β	[48]	[49]	[50]	Present study
0.0	—	0.469600	0.4696	0.469600
0.1	0.587035	0.587080	0.5870	0.587035
0.3	0.774755	0.774724	0.7748	0.774755
0.5	0.927680	0.927905	0.9277	0.927680
1.0	1.232585	1.238589	1.2326	1.232588
1.6	1.521514	1.518488	1.5215	1.521551

TABLE 2: Numerical values of $C_f \mathrm{Re}^{1/2}\sqrt{2/m+1}$ when $Lb = Rd = 1, \beta^* = Pe = Ec = Sc = 0.2, Pr = 7$, and $Nt = Nb = 0.1$.

A	n	We	M	β	λ	$C_f \mathrm{Re}^{1/2}\sqrt{(2/m+1)}$
0.2	0.2	1	0.1	0.1	0.3	0.618741
0.3						0.662672
0.4						0.705045
0.2	0.3					0.591906
	0.5					0.537024
	0.7					0.480843
	0.2	0.5				0.609744
		2				0.635470
		3				0.650840
		1	0.1			0.618741
			0.3			0.737507
			0.5			0.841418
			0.1	0.2		0.661328
				0.4		0.739924
				0.6		0.811700
				0.1	0.2	0.691738
					0.4	0.541350
					0.6	0.374491

Table 3: Numerical values of $Re_x^{-1/2} Nu_x \sqrt{2/m+1}$ for various parameters when $Lb = 1, n = 0.2, We = 1$, and $Sc = \beta^* = Pe = 0.2$.

A	Rd	Nb	Nt	M	Pr	β	Ec	λ	$Re_x^{-1/2} Nu_x \sqrt{(2/m+1)}$
0.1	1	0.1	0.1	0.1	7	0.1	0.2	0.3	4.264843
0.2									4.638632
0.3									4.989138
0.2	2								6.048218
	3								7.244505
	4								8.306865
	1	0.2							4.448489
		0.4							4.089907
		0.6							3.760368
		0.1	0.2						4.472414
			0.4						4.161547
			0.6						3.878221
			0.1	0.2					4.643489
				0.3					4.646502
				0.4					4.648149
				0.1	7				4.638676
					10				5.361452
					15				6.298947
					1	0.2			4.627500
						0.4			4.600568
						0.6			4.568220
						0.1	0.4		4.610188
							0.6		4.582073
							0.8		4.553956
							0.2	0.2	4.309568
								0.4	4.949331
								0.6	5.526109

Table 4: The numerical values $-Re_x^{-1/2} Sh_x \sqrt{2/m+1}$ for various parameters when $Lb = Rd = We = 1, Pr = 7$, and $\beta^* = Pe = Ec = n = 0.2$.

A	Nb	Nt	M	β	λ	$-Re_x^{-1/2} Sh_x \sqrt{(2/m+1)}$
0.1	0.1	0.1	0.1	0.1	0.3	0.726523
0.2						0.824367
0.3						0.914499
0.2	0.2					0.053217
	0.4					−0.329876
	0.6					−0.329901
	0.3	0.2				0.192495
		0.4				0.870622
		0.6				1.417330
		0.3	0.2			0.541510
			0.3			0.534349
			0.5			0.521425
			0.1	0.2		0.534660
				0.4		0.521431
				0.6		0.508467
				0.1	0.2	0.457287
					0.4	0.636060
					0.6	0.796142

each of Weissenberg number We, unsteadiness parameter A, Hartree pressure gradient β, and magnetic parameter M.

5.2. The Nusselt Number. The fluctuations in the heat transfer rate $Re_x^{-1/2} Nu_x \sqrt{2/m+1}$ caused by variation in important parameters are demonstrated in Table 3. The Nusselt number is enhanced as the values of the Prandtl number Pr, velocity ratio parameter λ, unsteadiness parameter A, the magnetic number M, and thermal radiation parameter Rd are hiked; however, it is depressed as thermophoresis parameter Nt, Hartree pressure gradient β, Brownian motion parameter Nb, and Eckert number Ec are increased.

TABLE 5: Numerical values of $\text{Re}_x^{-1/2} Nn_x \sqrt{2/m+1}$ for pertinent parameters when $Rd = We = 1, M = 0.1, Pr = 7$, and $A = Ec = n = 0.2$.

β	β^*	Sc	Pe	Lb	Nt	Nb	λ	$\text{Re}_x^{-1/2} Nn_x \sqrt{(2/m+1)}$
0.1	0.2	0.2	0.2	1	0.1	0.1	0.3	1.294224
0.2								1.286385
0.3								1.277968
0.1	0.4							1.260807
	0.6							1.227390
	0.8							1.193973
	0.2	0.5						1.378667
		1						1.470230
		2						1.595195
		1	0.2					1.378667
			0.5					1.243516
			1					1.018624
			0.2	2				2.029791
				3				2.455442
				4				2.812551
				2	0.2			1.892830
					0.4			1.707821
					0.6			1.610277
					0.3	0.2		2.024691
						0.4		2.140621
						0.6		2.176051
						0.3	0.2	2.005064
							0.4	2.196796
							0.6	2.374883

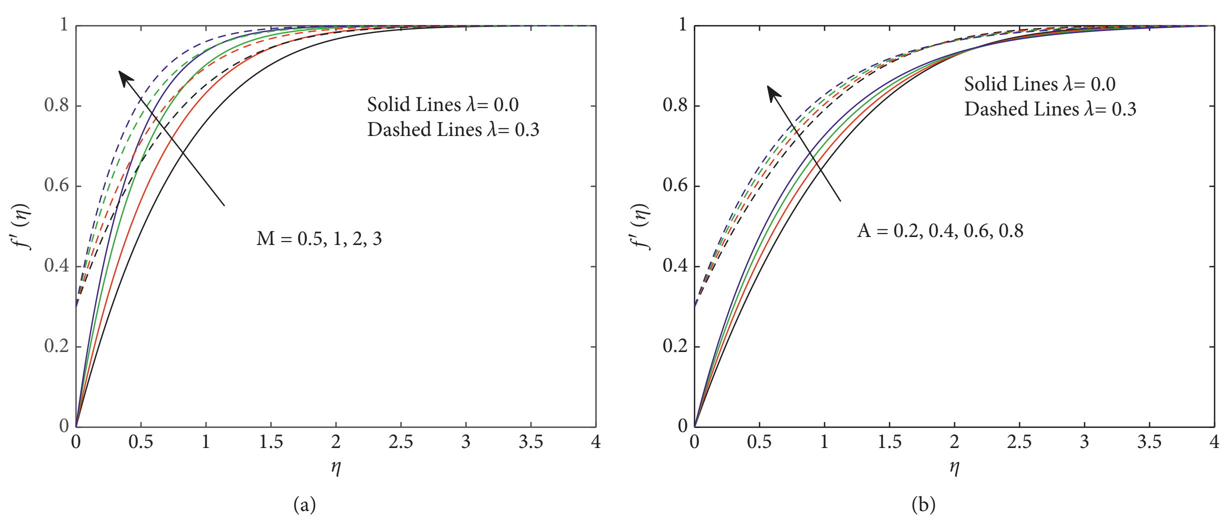

FIGURE 3: Fluctuations due to (a) M and (b) A in $f'(\eta)$.

5.3. The Sherwood Number. To visualize the fluctuations in the Sherwood number $-Re_x^{-1/2} Sh_x \sqrt{2/m+1}$ due to various pertinent parameters, Table 4 is displayed. The Sherwood number is enhanced for growing values of each of the unsteadiness parameter A, thermophoresis parameter Nt,and velocity ratio parameter λ while it is attenuated for the rising values of the magnetic parameter M, Hartree pressure gradient β, and Brownian motion parameter Nb.

5.4. The Density Number. Table 5 is represented to analyze the fluctuations in the density number $Re_x^{-1/2} Nn_x \sqrt{2/m+1}$ due to physical parameters. The gradually boosting values of the Schmidt number Sc, velocity ratio parameter λ, bio-convection Lewis parameter Lb, and Brownian motion parameter Nb cause an enhancement in the density number while it decreases as the micro-organism concentration difference parameter β^*, thermophoresis parameter Nt, Hartree pressure gradient β and Peclet number Pe are enhanced.

5.5. Graphical Results. In this section, the impact of governing parameters on flow field, energy, concentration, and density profile is sketched and discussed in detail. Both stretching and statics cases have been discussed.

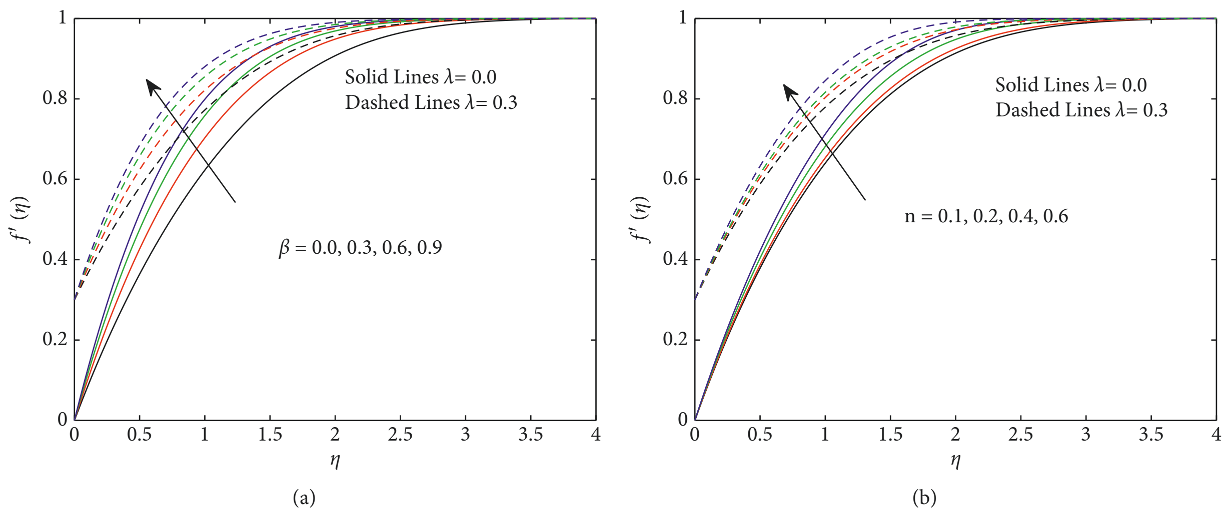

FIGURE 4: Fluctuations due to (a) β and (b) n in $f'(\eta)$.

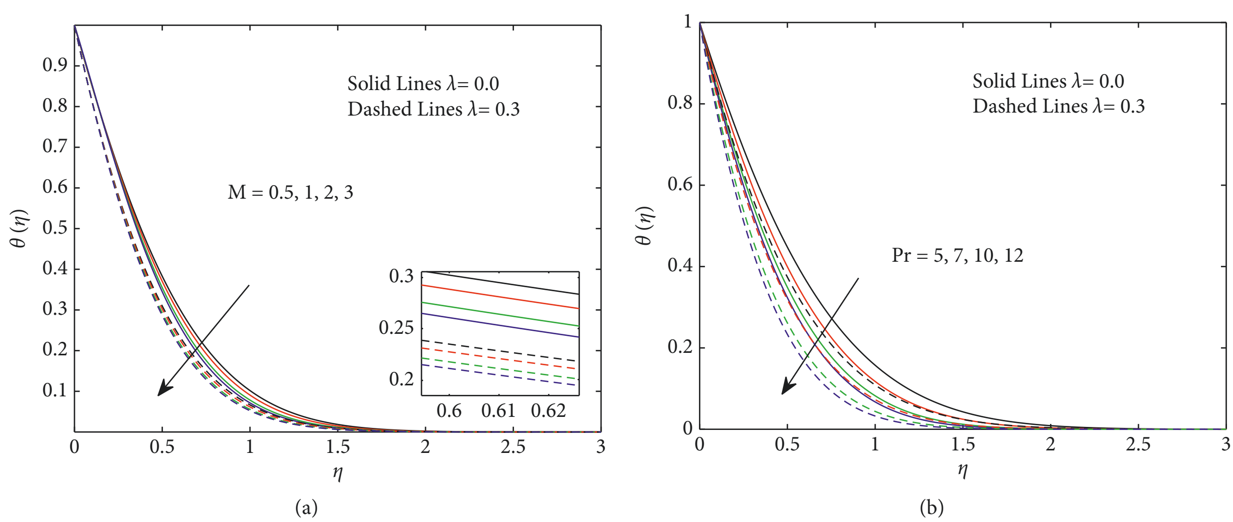

FIGURE 5: Fluctuations due to (a) M and (b) Pr in $\theta(\eta)$.

For graphical results, the involved parameters are allocated fixed values as $A = Pe = \beta^* = Ec = n = 0.2$, $We = Lb =, Rd = 1, M = \beta = Nb = Nt = 0.1 \mathrm{Pr} = 7$, and $\lambda = 0.3$ unless otherwise mentioned.

5.5.1. The Velocity Profile. To expose the impact of governing parameters on the velocity distribution $f'(\eta)$ of the tangent hyperbolic nanofluid, Figures 3(a), 3(b), 4(a), and 4(b) are displayed. Figures 3(a) and 3(b) are demonstrated to present the fluctuation in $f'(\eta)$ caused by the magnetic number M and unsteadiness parameter A. From this figure, it is evident that velocity profile $f'(\eta)$ is upsurged for the higher values of the magnetic number M and displayed in Figure 3(a). Increment in the magnetic number M means a decrement in the viscous force which lessens the momentum boundary layer thickness. Figure 3(b) is sketched to study the influence of unsteadiness parameter A on velocity profile $f'(\eta)$. The growing values of unsteadiness parameter A and velocity profile $f'(\eta)$ are enhanced whereas related boundary layer thickness becomes thinner. However, in case of stretching wedge, it is higher as compared with the static wedge. The influence of the wedge angle parameter β and power law index n on velocity distribution $f'(\eta)$ is captured in Figures 4(a) and 4(b). $\beta > 0$ addresses the accelerating flow, and it is an interesting fact that the boundary layer thickness is declined as β is hiked and fluid squeezes more closer to the wall surface, as presented in Figure 4(a). Figure 4(b) is divulged to study the impact of the power law index n. This figure shows that velocity profile $f'(\eta)$ is escalated for accelerating values of the power law index n

5.5.2. The Temperature Profile. The impact of sundry parameters on the temperature profile $\theta(\eta)$ is presented in Figures 5–7. Figures 5(a) and 5(b) portray the influence

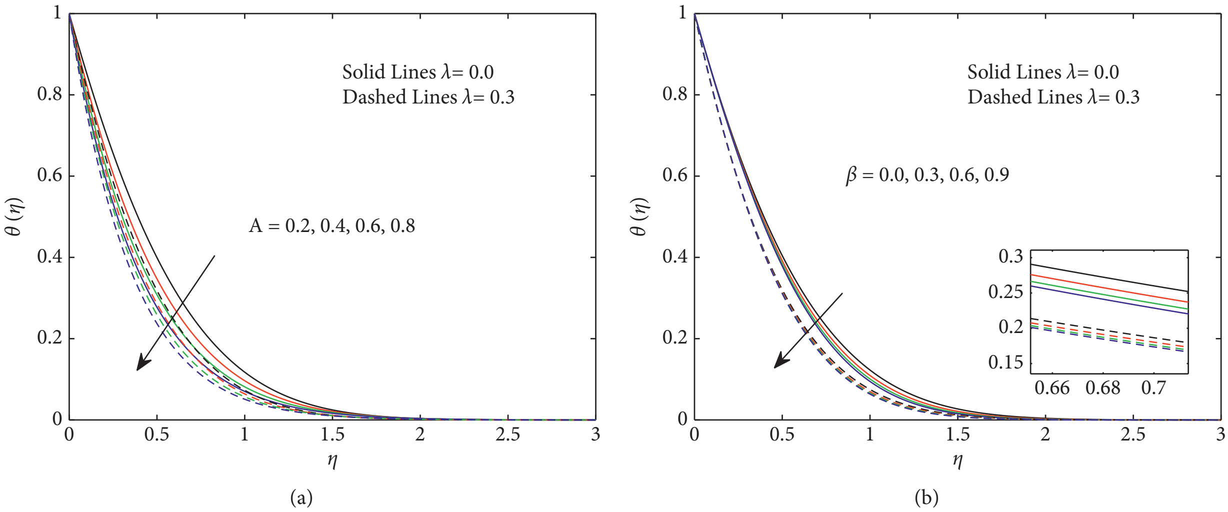

Figure 6: Fluctuations due to (a) A and (b) β in $\theta(\eta)$.

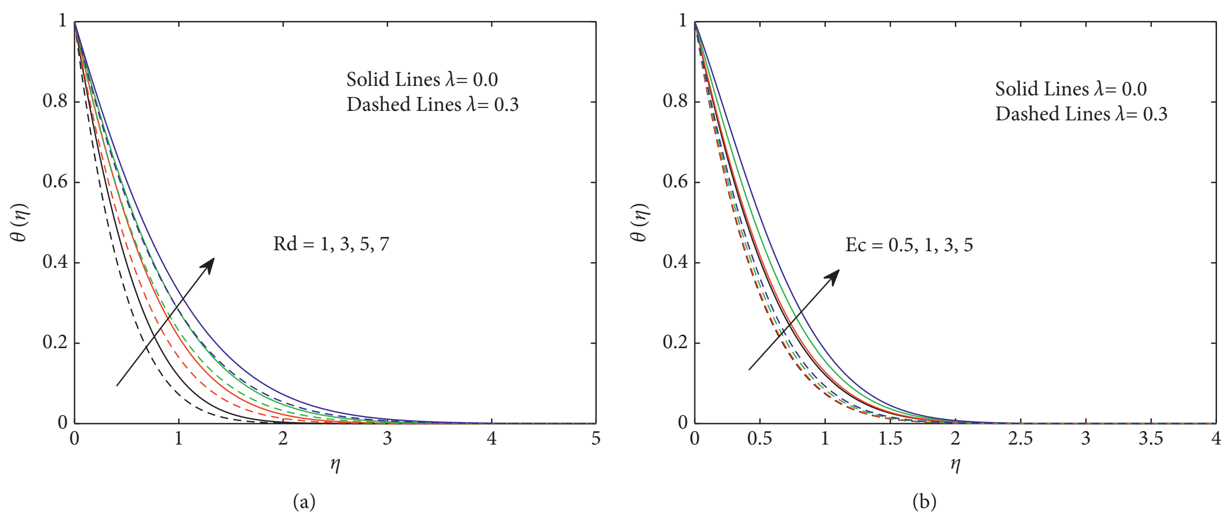

Figure 7: Fluctuations due to (a) Rd and (b) Ec in $\theta(\eta)$.

magnetic number M and Prandtl number Pr on temperature profile $\theta(\eta)$. A decreasing trend is noticed in temperature profile $\theta(\eta)$ as the values of the magnetic number M are escalated as displayed in Figure 5(a). Figure 5(b) reflects the impact Pr on the temperature distribution. The curves in this figure indicate that increasing the Prandtl number Pr causes a decline in the energy profile. Physically, increase in Pr reduces the effect of the thermal conductivity due to which temperature profile $\theta(\eta)$ reduces. Figure 6(a) reflects that the unsteadiness parameter A diminishes the temperature profile $\theta(\eta)$. Physically, when the unsteadiness parameter A is increased, the stretching sheet loses its heat due to which the temperature of the nanofluid is declined. To expose the behavior of β, Figure 6(b) is displayed. For the value $\beta = 0$, the temperature is maximum, and for the growing values of $\beta > 0$, the temperature profile is declined. The temperature distribution $\theta(\eta)$ is escalated as Rd gets bigger as shown in Figure 7(a). Physically, increment in temperature profile $\theta(\eta)$ strengthens the fact that more heat is produced due to the radiation process. The effect of viscous dissipation is presented by Eckert number Ec. It is a number that represents the relation between the kinetic energy and the change in enthalpy. The impact of the Eckert number Ec on temperature profile $\theta(\eta)$ is chalked out in Figure 7(b). It is noticed that as Ec grows, the energy profile $\theta(\eta)$ is boosted. Physically, as the dissipation is increased, the thermal conductivity improves which helps to increase the temperature profile $\theta(\eta)$.

5.5.3. The Concentration Profile. In order to study the variations in concentration distribution $\phi(\eta)$ due to the impact of sundry parameters, Figures 8(a) and 8(b) are presented. Figure 8(a) is chalked out to study the effect of unsteadiness parameter A on $\phi(\eta)$. A decrement in concentration distribution $\phi(\eta)$ is viewed for the higher values of unsteadiness parameter A. Figure 8(b) is demonstrated to view the effect of the Schmidt number Sc on $\phi(\eta)$. As the

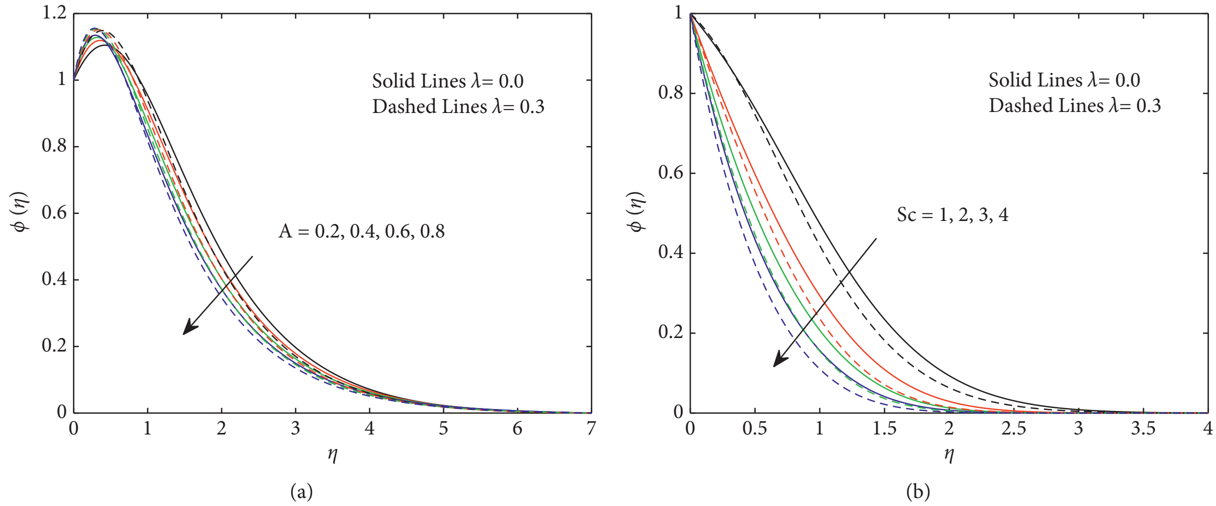

Figure 8: Variations due to (a) A and (b) Sc in $\phi(\eta)$.

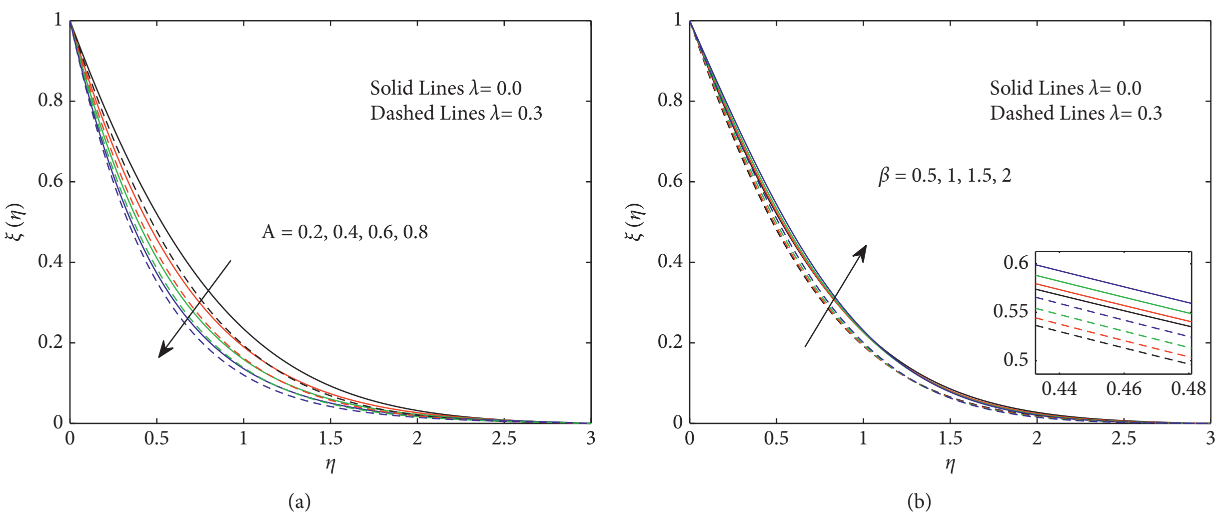

Figure 9: Variations due to (a) A and (b) β in $\xi(\eta)$.

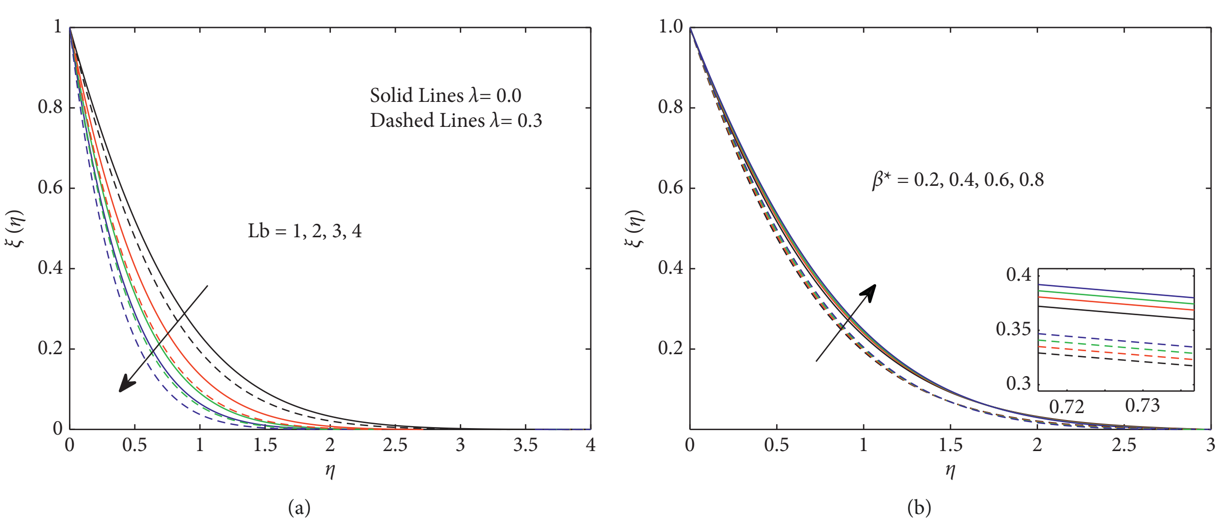

Figure 10: Variations due to (a) Lb and (b) β^* in $\xi(\eta)$.

Schmidt number Sc is upsurged, $\phi(\eta)$ is diminution. It is due to the fact that the mass diffusivity has inverse relation with the Schmidt number, therefore, the higher values of the Schmidt number bring weaker mass diffusion as a result nanoparticles concentration is dropped.

5.5.4. The Density Profile. The behavior of the motile density profile $\xi(\eta)$ due to emerging parameters is displayed in Figures 9(a), 9(b), 10(a), and 10(b). A diminution in motile density profile $\xi(\eta)$ is noticed as the unsteadiness parameter A is upsurged; however, it is mounted for an increment in the Hartree pressure gradient β as presented in Figures 9(a) and 9(b), respectively. A raise in bioconvection Lewis number Lb causes a decline in motile density profile $\xi(\eta)$ as portrayed in Figure 10(a). Physically, the diffusivity of the organism decreases as bioconvection Lewis number Lb is enhanced due to which motile density distribution $\xi(\eta)$ and relevant boundary layer thickness are declined. The influence of micro-organism concentration difference parameter β^* on motile density profile $\xi(\eta)$ is demonstrated in Figure 10(b). The motile density distribution $\xi(\eta)$ is augmentation for growing values of micro-organism concentration difference parameter β^*. However, it is smaller in case of stretching wedge as compared with static wedge.

6. Conclusions

In the present article, numerical investigation of tangent hyperbolic nanofluid flow over a wedge-shaped surface in the presence of micro-organisms has been presented. Few of the important results are as follows:

(i) The skin friction is enhanced whereas the motile density number is vitiated for larger values of the Hartree pressure gradient β

(ii) The Nusselt number, skin friction coefficient, and Sherwood number are increased as the unsteadiness parameter A gets bigger

(iii) The velocity profile is increased for the growing values of the magnetic number M and the unsteadiness parameter A

(iv) The energy and concentration distribution are diminished for the escalating values of the unsteadiness parameter A

(v) The density field is attenuated as unsteadiness parameter A and the bioconvection Lewis number Lb are increased but reverse behavior is noticed for the micro-organism concentration difference parameter β^* and the Hartree pressure gradient β

Abbreviations

$A = c/ax^{m-1}$:	The unsteadiness parameter
B_0:	Applied magnetic field
C_∞:	Ambient concentration
C:	Boundary layer concentration
C_p:	Specific heat
C_f:	Skin friction coefficient
C_0:	Initial reference concentration
C_w:	Concentration at wall surface
D_T:	Thermophoresis diffusion parameter
D_B:	Brownian diffusion coefficient
$Ec = U_w^2/(C_p)_f(T_w - T_\infty)$:	Eckert number
h_w:	Local surface heat flux
n:	Thermal conductivity
Lb:	Bioconvection Lewis number
$M = \sigma B_0^2/a\rho xm - 1$:	Magnetic number
k:	The power law index
N:	Boundary layer micro-organism
N_0:	Initial micro-organism concentration
N_w:	Micro-organisms at wall surface
Nu_x:	Nusselt number
$Nt = \Lambda D_T(T_w - T_\infty)/\nu T_\infty$:	Thermophoresis parameter
$Nb = \Lambda D_B(C_w - C_\infty)/\nu$:	Brownian motion parameter
$Pr = \nu/\alpha$:	Prandtl number
$Pe = bW_c/D_n$:	The bioconvection Peclet number
$Rd = 4\sigma^* T_\infty^3/k\kappa^*$:	Thermal radiation parameter
q_r:	Radiative heat flux
$Sc = \nu/D_B$:	The Schmidt number
t:	Time
T_w:	Surface temperature
T:	Boundary layer temperature
T_0:	Initial reference temperature
kT_∞:	Ambient temperature
u, v:	Velocity components
u_w:	Characteristics velocity
$We = \sqrt{\Gamma^2(m+1)U_e^3/\nu x}$:	The Weissenberg number.

Greek Symbols

ν:	Kinematic viscosity
ρ:	Fluid density
μ:	Dynamic viscosity
σ_m:	Electric charge density
φ:	Dimensionless concentration
θ:	Dimensionless temperature
$(\rho C_p)_f$:	Heat capacity of the fluid
$(\rho C_p)_p$:	Heat capacity of the nanoparticles $\Lambda = (\rho C_p)_p/(\rho C_p)_f$
η:	Dimensionless boundary layer thickness
λ:	The velocity ratio parameter
$\beta = m/m + 2$:	Hartree pressure gradient
$\beta^* = N_\infty/N_w - N_\infty$:	Micro-organism concentration difference parameter.

Data Availability

No data were used to support this study.

Conflicts of Interest

The authors declare that they have no conflicts of interest.

References

[1] S. U. S. Choi, "Development and application of non-Newtonian flows," *American Society of Mechanical Engineers (ASME)*, vol. 231, pp. 99–105, 1995.

[2] S. Lee, S. U.-S. Choi, S. Li, and J. A. Eastman, "Measuring thermal conductivity of fluids containing oxide nanoparticles," *Journal of Heat Transfer*, vol. 121, no. 2, pp. 280–289, 1999.

[3] J. A. Eastman, S. U. S. Choi, S. Li, W. Yu, and L. J. Thompson, "Anomalously increased effective thermal conductivities of ethylene glycol-based nanofluids containing copper nanoparticles," *Applied Physics Letters*, vol. 78, no. 6, pp. 718–720, 2001.

[4] M. Sheikholeslami, S. A. Shehzad, Z. Li, and A. Shafee, "Numerical modeling for alumina nanofluid magnetohydrodynamic convective heat transfer in a permeable medium using Darcy law," *International Journal of Heat and Mass Transfer*, vol. 127, pp. 614–622, 2018.

[5] H. Goodarzi, O. A. Akbari, M. M. Sarafraz, M. M. Karchegani, M. R. Safaei, and G. A. Sheikh Shabani, "Numerical simulation of natural convection heat transfer of nanofluid with Cu MWCNT and Al_2O_3," *Journal of Thermal Science and Engineering Applications*, vol. 11, no. 6, 2019.

[6] H. Mondal, S. Mishra, P. K. Kundu, and P. Sibanda, "Entropy generation of variable viscosity and thermal radiation on magneto nanofluid flow with dusty fluid," *Journal of Applied and Computational Mechanics*, vol. 6, no. 1, pp. 171–182, 2020.

[7] T. Khamliche, S. Khamlich, T. B. Doyle, D. Makinde, and M. Maaza, "Thermal conductivity enhancement of nano-silver particles dispersed ethylene glycol based nanofluids," *Materials Research Express*, vol. 5, no. 3, Article ID 35020, 2018.

[8] Z. Nisar, T. Hayat, A. Alsaedi, and B. Ahmad, "Significance of activation energy in radiative peristaltic transport of Eyring-Powell nanofluid," *International Communications in Heat and Mass Transfer*, vol. 116, p. 104655, 2020.

[9] R. Ellahi, F. Hussain, S. Asad Abbas, M. M. Sarafraz, M. Goodarzi, and M. S. Shadloo, "Study of two-phase Newtonian nanofluid flow hybrid with Hafnium particles under the effects of slip," *Inventions*, vol. 5, no. 1, 2020.

[10] M. M. Sarafraz and F. C. Christo, "Phase change heat transfer induced by plasmon heat generation in liquid micro-layer inside a micro-reactor," *Journal of Energy Storage*, vol. 42, Article ID 103033, 2021.

[11] W. Ibrahim and A. Tulu, "Magnetohydrodynamic (MHD) boundary layer flow past a wedge with heat transfer and viscous effects of nanofluid embedded in porous media," *Mathematical Problems in Engineering*, vol. 2019, Article ID 4507852, 2019.

[12] S. M. Atif, S. Hussain, and M. Sagheer, "Heat and mass transfer analysis of time-dependent tangent hyperbolic nanofluid flow past a wedge," *Physics Letters A*, vol. 383, no. 11, pp. 1187–1198, 2019.

[13] D. Ibrahim, M. Daba, and S. Bati, "Optimal Homotopy asymptotic method for investigation of effects of thermal radiation, internal heat generation, and buoyancy on velocity and heat transfer in the Blasius flow," *Mathematical Problems in Engineering*, vol. 2021, Article ID 5598817, 2021.

[14] S. Yousefzadeh, H. Rajabi, N. Ghajari, M. M. Sarafraz, O. A. Akbari, and M. Goodarzi, "Numerical investigation of mixed convection heat transfer behavior of nanofluid in a cavity with different heat transfer areas," *Journal of Thermal Analysis and Calorimetry*, vol. 140, no. 6, pp. 2779–2803, 2020.

[15] S. M. Atif, S. Hussain, and M. Sagheer, "Effect of thermal radiation and variable thermal conductivity on magnetohydrodynamics squeezed flow of Carreau fluid over a sensor surface," *Journal of Nanofluids*, vol. 8, no. 4, pp. 806–816, 2019.

[16] C. S. Sravanthi and R. S. R. Gorla, "Effects of heat source/sink and chemical reaction on MHD Maxwell nanofluid flow over a convectively heated exponentially stretching sheet using homotopy analysis method," *International Journal of Applied Mechanics and Engineering*, vol. 23, no. 1, pp. 137–159, 2018.

[17] M. Raza, R. Ellahi, S. M. Sait, M. M. Sarafraz, M. S. Shadloo, and I. Waheed, "Enhancement of heat transfer in peristaltic flow in a permeable channel under induced magnetic field using different CNTs," *Journal of Thermal Analysis and Calorimetry*, vol. 140, no. 3, pp. 1277–1291, 2020.

[18] M. M. Sarafraz and F. C. Christo, "Thermal and flow characteristics of liquid flow in a 3D-printed micro-reactor: a numerical and experimental study," *Applied Thermal Engineering*, vol. 199, Article ID 117531, 2021.

[19] A. F. Elelamy, N. S. Elgazery, and R. Ellahi, "Blood flow of MHD non-Newtonian nanofluid with heat transfer and slip effects," *International Journal of Numerical Methods for Heat and Fluid Flow*, vol. 30, no. 11, pp. 4883–4908, 2020.

[20] S. M. Atif, A. Kamran, and S. Shah, "MHD micropolar nanofluid with non Fourier and non Fick's law," *International Communications in Heat and Mass Transfer*, vol. 122, Article ID 105114, 2021.

[21] S. Chakraborty and P. K. Panigrahi, *Stability of Nanofluid: A Review*, Applied Thermal Engineering, Amsterdam, Netherlands, 2020.

[22] S. Nazari, R. Ellahi, M. M. Sarafraz, M. R. Safaei, A. Asgari, and O. A. Akbari, "Numerical study on mixed convection of a non-Newtonian nanofluid with porous media in a two lid-driven square cavity," *Journal of Thermal Analysis and Calorimetry*, vol. 140, no. 3, pp. 1121–1145, 2020.

[23] S. M. Atif, M. Abbas, U. Rashid, and H. Emadifar, "Stagnation point flow of EMHD micropolar nanofluid with mixed convection and slip boundary," *Complexity*, vol. 2021, Article ID 3754922, 2021.

[24] M. Y. Malik, T. Salahuddin, A. Hussain, and S. Bilal, "MHD flow of tangent hyperbolic fluid over a stretching cylinder: using Keller box method," *Journal of Magnetism and Magnetic Materials*, vol. 395, pp. 271–276, 2015.

[25] R. Ellahi, S. Z. Alamri, A. Basit, and A. Majeed, "Effects of MHD and slip on heat transfer boundary layer flow over a moving plate based on specific entropy generation," *Journal of Taibah University for Science*, vol. 12, no. 4, pp. 476–482, 2018.

[26] K. Jabeen, M. Mushtaq, and R. M. Akram, "Analysis of the MHD boundary layer flow over a nonlinear stretching sheet in a porous medium using semianalytical approaches," *Mathematical Problems in Engineering*, vol. 2020, Article ID 3012854, 2020.

[27] M. Ramzan, H. Gul, J. D. Chung, S. Kadry, and Y.-M. Chu, "Significance of Hall effect and Ion slip in a three-dimensional bioconvective tangent hyperbolic nanofluid flow subject to Arrhenius activation energy," *Scientific Reports*, vol. 10, no. 1, pp. 18342–18357, 2020.

[28] P. P. Gharami, S. Reza-E-Rabbi, S. M. Arifuzzaman, M. S. Khan, T. Sarkar, and S. F. Ahmmed, "MHD effect on unsteady flow of tangent hyperbolic nano-fluid past a moving

cylinder with chemical reaction," *SN Applied Sciences*, vol. 2, no. 7, p. 1256, 2020.
[29] A. Shafiq, S. A. Lone, T. N. Sindhu, Q. M. Al-Mdallal, and G. Rasool, "Statistical modeling for bioconvective tangent hyperbolic nanofluid towards stretching surface with zero mass flux condition," *Scientific Reports*, vol. 11, no. 1, pp. 13869–13880, 2021.
[30] M. A. Yousif, H. F. Ismael, T. Abbas, and R. Ellahi, "Numerical study of momentum and heat transfer of MHD Carreau nanofluid over an exponentially stretched plate with internal heat source/sink and radiation," *Heat Transfer Research*, vol. 50, no. 7, pp. 649–658, 2019.
[31] S. Shah, S. M. Atif, and A. Kamran, "Radiation and slip effects on MHD Maxwell nanofluid flow over an inclined surface with chemical reaction," *Heat Transfer*, vol. 50, no. 4, pp. 4062–4085, 2021.
[32] S. Rashidi, M. Dehghan, R. Ellahi, M. Riaz, and M. T. Jamal-Abad, "Study of stream wise transverse magnetic fluid flow with heat transfer around an obstacle embedded in a porous medium," *Journal of Magnetism and Magnetic Materials*, vol. 378, pp. 128–137, 2015.
[33] S. M. Atif, S. Hussain, and M. Sagheer, "Effect of viscous dissipation and Joule heating on MHD radiative tangent hyperbolic nanofluid with convective and slip conditions," *Journal of the Brazilian Society of Mechanical Sciences and Engineering*, vol. 41, no. 4, pp. 189–206, 2019.
[34] R. Ellahi, R. S.U., S. Nadeem, and V. K, "The blood flow of Prandtl fluid through a tapered stenosed arteries in permeable walls with magnetic field," *Communications in Theoretical Physics*, vol. 63, no. 3, pp. 353–358, 2015.
[35] M. S. Kandelousi and R. Ellahi, "Simulation of ferrofluid flow for magnetic drug targeting using the lattice Boltzmann method," *Zeitschrift für Naturforschung A*, vol. 70, no. 2, pp. 115–124, 2015.
[36] Z. Ullah, G. Zaman, and A. Ishak, "Magnetohydrodynamic tangent hyperbolic fluid flow past a stretching sheet," *Chinese Journal of Physics*, vol. 66, pp. 258–268, 2020.
[37] S. M. Atif, S. Hussain, and M. Sagheer, "Numerical study of MHD micropolar Carreau nanofluid in the presence of induced magnetic field," *AIP Advances*, vol. 8, 2018.
[38] H. Xu and J. Cui, "Mixed convection flow in a channel with slip in a porous medium saturated with a nanofluid containing both nanoparticles and microorganisms," *International Journal of Heat and Mass Transfer*, vol. 125, pp. 1043–1053, 2018.
[39] D. Pal and S. K. Mondal, "Influence of chemical reaction and nonlinear thermal radiation on bioconvection of nanofluid containing gyrotactic microorganisms with magnetic field," *BioNanoScience*, vol. 8, no. 4, pp. 1065–1080, 2018.
[40] S. M. Atif, S. Hussain, and M. Sagheer, "Magnetohydrodynamic stratified bioconvective flow of micropolar nanofluid due to gyrotactic microorganisms," *AIP Advances*, vol. 9, 2019.
[41] M. Zhao, Y. Xiao, and S. Wang, "Linear stability of thermal-bioconvection in a suspension of gyrotactic micro-organisms," *International Journal of Heat and Mass Transfer*, vol. 126, pp. 95–102, 2018.
[42] S. Saini and Y. D. Sharma, "Analysis of onset of bio-thermal convection in a fluid containing gravitactic microorganisms by the energy method," *Chinese Journal of Physics*, vol. 56, no. 5, pp. 2031–2038, 2018.
[43] K. Al-Khaled, S. U. Khan, and I. Khan, "Chemically reactive bioconvection flow of tangent hyperbolic nanoliquid with gyrotactic microorganisms and nonlinear thermal radiation," *Heliyon*, vol. 6, 2020.
[44] S. Sarkar and M. F. Endalew, "Effects of melting process on the hydromagnetic wedge flow of a Casson nanofluid in a porous medium," *Boundary Value Problems*, vol. 43, 2019.
[45] C. S. K. Raju, M. M. Hoque, and T. Sivasankar, "Radiative flow of Casson fluid over a moving wedge filled with gyrotactic microorganisms," *Advanced Powder Technology*, vol. 28, no. 2, pp. 575–583, 2017.
[46] E. Fatunmbi and A. Adeniyan, "MHD stagnation point-flow of micropolar fluids past a permeable stretching plate in porous media with thermal radiation, chemical reaction and viscous dissipation," *Journal of Advances in Mathematics and Computer Science*, vol. 26, no. 1, pp. 1–19, 2018.
[47] K. G. Kumar, B. J. Gireesha, and R. S. R. Gorla, "Flow and heat transfer of dusty hyperbolic tangent fluid over a stretching sheet in the presence of thermal radiation and magnetic field," *International Journal of Mechanical and Materials Engineering*, vol. 13, 2018.
[48] K. R. Rajagopal, A. S. Gupta, and T. Y. Na, "A note on the Falkner-Skan flows of a non-Newtonian fluid," *International Journal of Non-linear Mechanics*, vol. 18, no. 4, pp. 313–320, 1983.
[49] B. L. Kuo, "Application of the differential transformation method to the solutions of Falkner-Skan wedge flow," *Acta Mechanica*, vol. 164, no. 2-3, pp. 161–174, 2003.
[50] A. Ishak, R. Nazar, and I. Pop, "Falkner-Skan equation for flow past a moving wedge with suction or injection," *Journal of Applied Mathematics and Computing*, vol. 25, no. 1-2, pp. 67–83, 2007.